BIOPROBES 77

JOURNAL OF CELL BIOLOGY APPLICATIONS

MAY 2018

Immuno-oncology: Advances in basic research and translational medicine

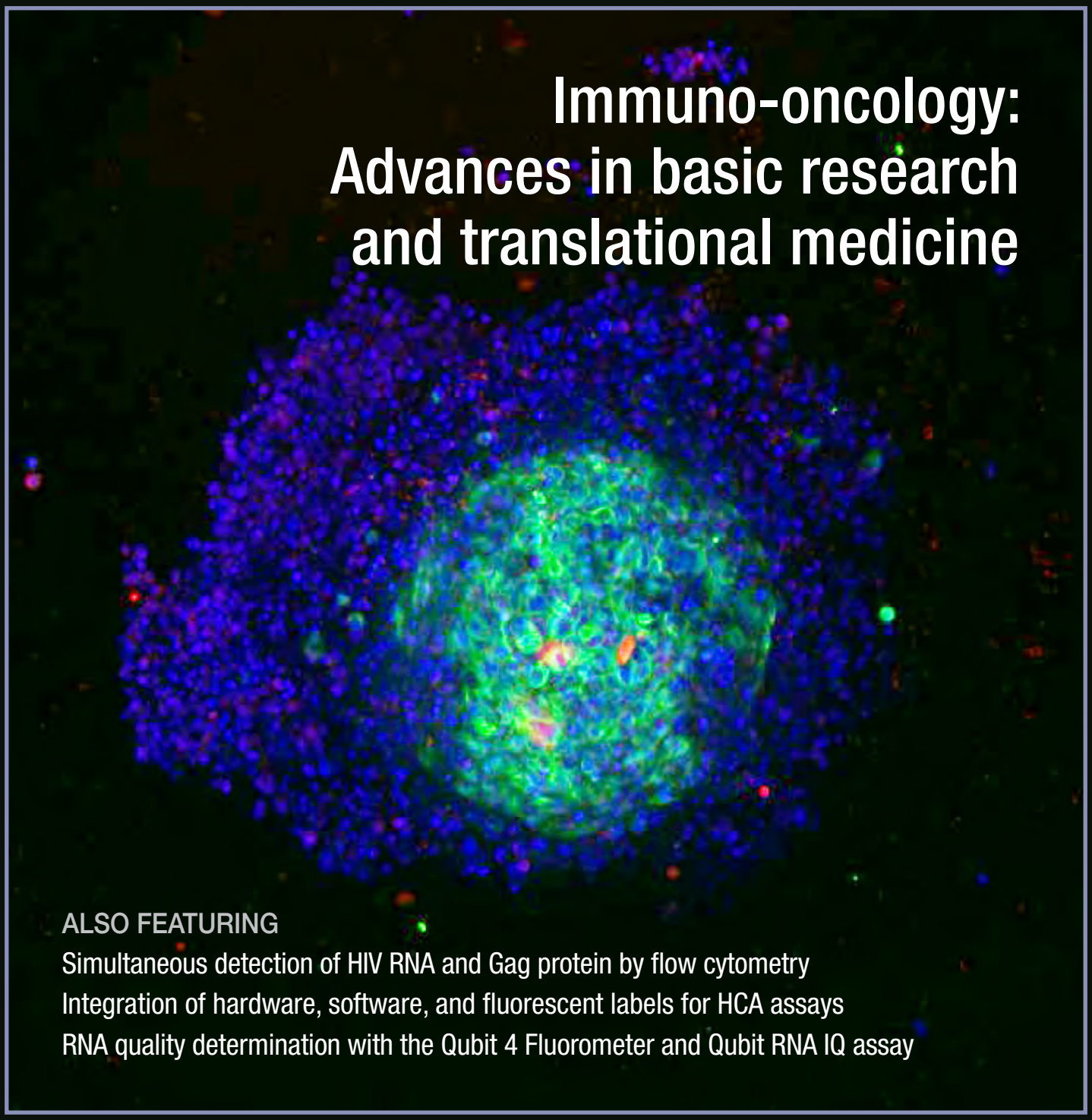

ALSO FEATURING

Simultaneous detection of HIV RNA and Gag protein by flow cytometry

Integration of hardware, software, and fluorescent labels for HCA assays

RNA quality determination with the Qubit 4 Fluorometer and Qubit RNA IQ assay

invitrogen
by Thermo Fisher Scientific

invitrogen

Countess II Automated Cell Counters

Fast | Accurate | Affordable

With a reusable slide option, Invitrogen™ Countess™ II Automated Cell Counters help bring more accurate and faster cell counting within reach.

Automate today at **thermofisher.com/cellcounting**

ThermoFisher SCIENTIFIC

BioProbes 77

invitrogen

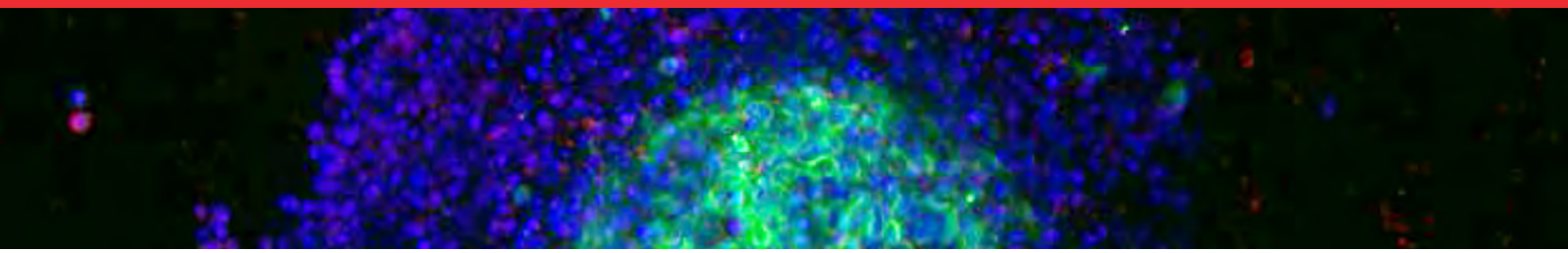

thermofisher.com/bioprobes • May 2018

Production Manager
Beth Browne

Editors
Michelle Spence
Grace Richter

Designer
Kim McGovern

Contributors
Laura Allred
Brian Almond
Suda Balasubramanian
John Bauer
Lisa Birkby
Ryan Bomgarden
Jolene Bradford
Beth Browne
Suzanne Buck
Gayle Buller
Nick Dolman
Sarvani Emani
Helen Fleisig
Kathleen Free
Nico Garcia
Oggie Golub
Tibor Henseler
Ridley Jacobs
Kamran Jamil
Greg Kaduchak
Kevin Kepple
Chris Langsdorf
Victoria Love
Bhaskar Mandavilli
Aya Miura
Monica O'Hara-Noonan
Priya Rangaraj
Sreethu Sankar
Patricia Sardina
Laura Shapiro
Basile Siewe
Haripriya Sridharan
Priyanka Swamynathan

BioProbes Journal, available in print and online at **thermofisher.com/bioprobes**, is dedicated to providing researchers with the very latest information about cell biology products and their applications. For a complete list of our products, along with extensive descriptions and literature references, please see our website.

ThermoFisher SCIENTIFIC

Immuno-oncology research: Flow cytometry resources for the fight against cancer

Immuno-oncologists today are actively investigating the tumor microenvironment, dissecting immune checkpoints, and developing precision therapies such as chimeric antigen receptor (CAR) T cells. By combining flow cytometry reagents and instruments, researchers can generate more complete and complex information about the immune system's role in cancer. Visit "Immuno-oncology research using flow cytometry" at **thermofisher.com/flow-io** for more information on sample preparation, flow cytometry antibodies, cell health assays, and flow cytometry platforms.

While there, you can also request a downloadable or printed version of the immuno-oncology flow cytometry guide "Empowering technologies for immuno-oncology research". This 24-page guide reviews several key areas of cancer research and provides simplified workflows for flow cytometry, biomarker profiling, and cell imaging.

On-demand webinar: "The complex pharmacology of T cell CARs"

Also on the "Immuno-oncology research using flow cytometry" webpage, you can find an on-demand webinar, "The complex pharmacology of T cell CARs", presented by Charles Prussak, PhD, Director of the Cell Therapy Translational Laboratory at the University of California, San Diego. In this webinar, Dr. Prussak discusses next-generation cell-based immunotherapies targeting cancer cells, and the current work in his lab to develop chimeric antigen receptor (CAR)–modified T cells that target the fetal antigen ROR1 (expected to enter phase I clinical studies in 2018). He focuses on:

- CAR T cell therapies and the impact that the production process can have on the clinical activities of these agents
- Toxicities that are most commonly observed when employing CD19-directed CAR T cell therapies, and the clinical interventions used to ameliorate these side effects
- Pivotal clinical trial results that were used as the basis for approval of tisagenlecleucel
- Next-generation CAR T cell therapies for the treatment of both hematological and solid-tumor malignancies

Access this on-demand cancer research webinar by Dr. Prussak at **thermofisher.com/flow-io**.

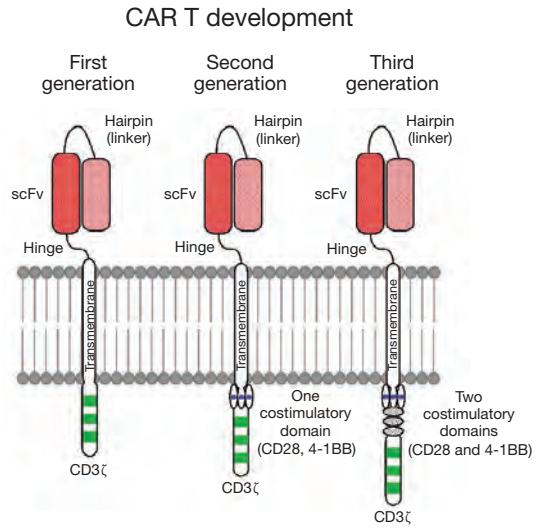

Boost synaptic strength: Complete a protein and cell analysis eLearning course

Would you like to learn about or review important protein and cell analysis application areas? We have produced a series of free, self-paced, animated courses that include knowledge checks and practical application exercises to help you solidify what you have learned, as well as downloadable course materials and relevant supplementary resources. Available courses include:

- Antibodies: Antibody validation*
- Flow cytometry: T cell stimulation and proliferation
- Protein biology: Protein sample preparation

All content is available 24 hours a day, 7 days a week, and is viewable from the convenience of your computer or mobile device. Find our latest eLearning course offerings at **thermofisher.com/elearningcourses**.

*The use or any variation of the word "validation" refers only to research-use antibodies that were subject to functional testing to confirm that the antibody can be used with the research techniques indicated. It does not ensure that the product or products were validated for clinical or diagnostic uses.

Instrument evaluation guide and webpage

Visit the "Considerations when purchasing a flow cytometer" webpage to learn more about how various capabilities of a flow cytometry instrument can enhance your research. This flow cytometry instrument evaluation focuses on the fluidic and optical systems, variations in the way technical specifications are calculated, and the importance of instrument maintenance, allowing you to explore how design features and software capabilities support your applications and sample types.

While on the flow cytometry instrument evaluation webpage, you can request a downloadable or printed version of the "Flow cytometer evaluation guide: Informed purchasing decisions through understanding experimental design and instrument capabilities". This 40-page guide discusses the fluidic and optical components and capabilities of various flow cytometers to facilitate objective comparisons of instruments from several manufacturers. It was developed in consultation with experts in mechanical, optical, systems, and software engineering, and it incorporates observations of researchers who perform flow cytometry workflows on a daily basis. Decide for yourself at **thermofisher.com/compareflow**.

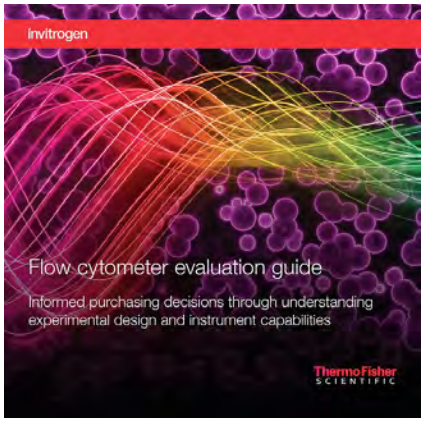

3D instrument tour for the Attune NxT Flow Cytometer

The Invitrogen™ Attune™ NxT Flow Cytometer makes multiparametric flow cytometry available to both new and experienced researchers. Designed for faster experimental run times, this compact flow cytometer uses acoustics-assisted hydrodynamic focusing technology to provide rapid and accurate analysis for a broad range of sample types.

Now you can take an online 3D instrument tour of the Attune NxT Flow Cytometer and Autosampler, available in 8 different languages (Japanese, Chinese, German, Spanish, French, Italian, Portuguese, and English). To begin your exploration of the fluidic and optical systems, software features, customer testimonials, and representative data for the Attune NxT Flow Cytometer, simply select the "3D Demo" button at **thermofisher.com/attune** and choose a language.

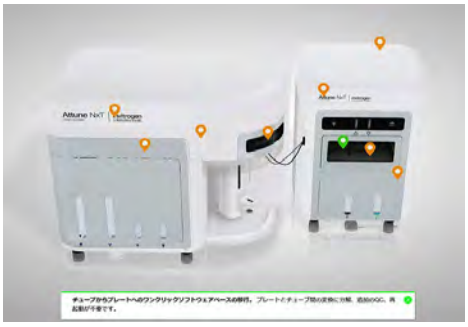

Helpful online resources for protein assays

Protein quantitation is an integral part of many laboratory workflows and often a necessary step before isolation, separation, and analysis by chromatography, electrophoresis, or immunochemical techniques. Thermo Scientific™ Pierce™ protein assays provide exceptional accuracy, compatibility, and broad applicability that enable most laboratory protein samples to be quantified with ease.

For help with identifying, comparing, and choosing the best protein assay for your specific application, we've created an online, interactive Protein Assay Selection Guide, which can be found at **thermofisher.com/proteinassayselectionguide**. Here you can filter and compare selections based on sample type, assay time, readout (colorimetric or fluorescent), and compatibility (with detergents or reducing agents). Then you're just a few friendly clicks away from finding the optimal protein assay for improved protein quantitation results.

You can also learn more about the latest advances in protein quantitation assays in a recently released white paper that provides key data on the linearity, protein-to-protein variation, and reagent compatibility of the Thermo Scientific™ Pierce™ Rapid Gold BCA Protein Assay. This two-component, detergent-compatible colorimetric assay provides the high sensitivity and linearity associated with the BCA assay, but in a fraction of the time it takes to perform a standard BCA assay. See our complete selection of BCA colorimetric protein assays and download a free copy of the white paper at **thermofisher.com/bca-assays**.

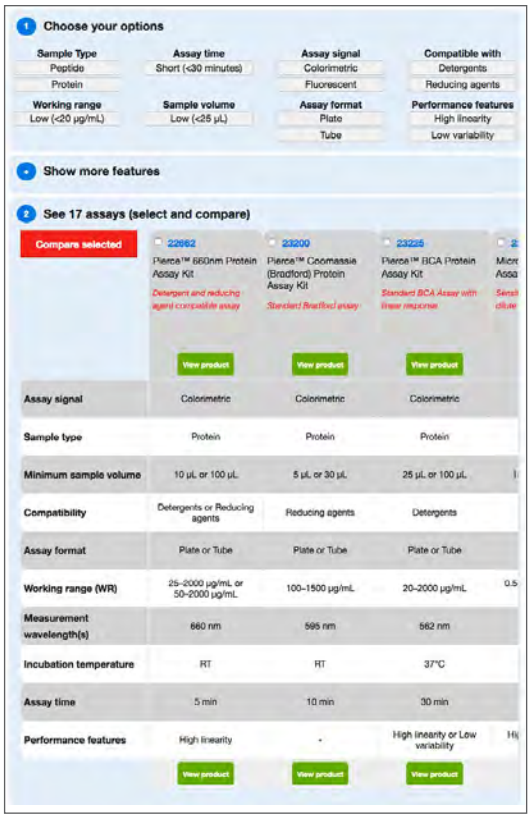

Direct-to-sample apoptotic cell stains for flow cytometry

Invitrogen™ Annexin V Ready Flow™ conjugates are ready-to-use, direct-to-sample apoptotic cell stains for labeling cells prior to analysis of apoptosis by flow cytometry. They require no dilution or pipetting, and are stable at room temperature. Simply add 1 drop directly to 10^5 cells in Ca^{2+}-containing buffer, incubate, and analyze. Fluorescent annexin V conjugates exhibit high affinity for phosphatidylserine (PS), which becomes exposed on the outer leaflet of cells undergoing apoptosis. See the complete line of Ready Flow reagents for apoptosis, cell cycle, and dead-cell identification at **thermofisher.com/readyflow**.

Product	Quantity	Cat. No.
Annexin V Alexa Fluor™ 488 Ready Flow™ Conjugate	120 reactions	R37174
Annexin V Alexa Fluor™ 647 Ready Flow™ Conjugate	120 reactions	R37175
Annexin V APC Ready Flow™ Conjugate	120 reactions	R37176
Annexin V Pacific Blue™ Ready Flow™ Conjugate	120 reactions	R37177

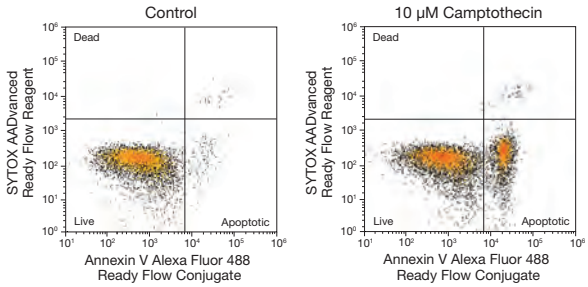

Extracellular phosphatidylserine detection in apoptotic cells using annexin V conjugates. Jurkat cells were treated with vehicle (left panel) or 10 µM camptothecin (right panel) for 3 hr and then stained with 1 drop of Invitrogen™ Annexin V Alexa Fluor™ 488 Ready Flow™ Conjugate (Cat. No. R37174) per 1 x 10^5 cells in 100 µL of annexin binding buffer. After cells were incubated for 15 min at 25°C, 400 µL annexin binding buffer was added along with 1 drop of Invitrogen™ SYTOX™ AADvanced™ Ready Flow Reagent (Cat. No. R37173), and data were acquired on an Invitrogen™ Attune™ NxT Flow Cytometer. Approximately 29% of the analyzed population stained positive with the annexin V conjugate in the camptothecin-treated sample.

Swap your Brilliant Violet 786 antibodies for Super Bright 780 antibodies

Invitrogen™ eBioscience™ Super Bright 780 antibody conjugates offer more options in marker and clone selection when you need a violet laser–excitable antibody conjugate for your flow cytometry experiment. Compared with Brilliant Violet™ 786 antibody conjugates, Super Bright 780 conjugates have less spillover into other violet channels and are compatible with standard intracellular buffers, viability stains, compensation beads, and other antibodies. The growing Super Bright antibody conjugate portfolio includes over 860 antibodies in five fluorophore formats. View the Super Bright selection guide, see comparative data, and select the Super Bright antibody conjugate for your next panel at **thermofisher.com/superbright**.

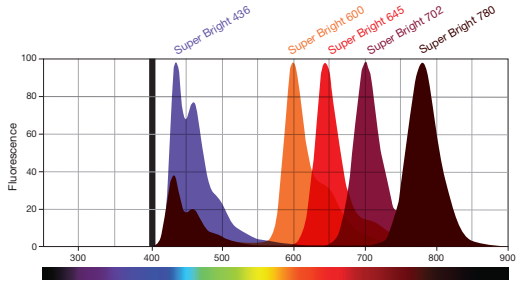

Emission spectra of Super Bright 436, Super Bright 600, Super Bright 645, Super Bright 702, and Super Bright 780 antibody conjugates. The less intense brown curve under the blue emission curve shows the contribution of the (donor) Super Bright 436 dye to the emission curves of the four longer-wavelength tandem Super Bright dyes.

GFP compensation for flow cytometry

Invitrogen™ GFP BrightComp eBeads™ Compensation Beads provide a reliable, accurate, and simple-to-use technique for setting flow cytometry compensation when using GFP-expressing samples. The single-color fluorescent beads are excited with a blue (488 nm) laser and exhibit three intensity levels to match a variety of GFP expression levels, with an emission spectrum nearly identical to that of GFP. These polystyrene beads—provided in a dropper bottle containing the spectrally matched fluorescent beads as well as the negative control beads—are dispensed as a single drop to the sample. Find out more at **thermofisher.com/brightcomp**.

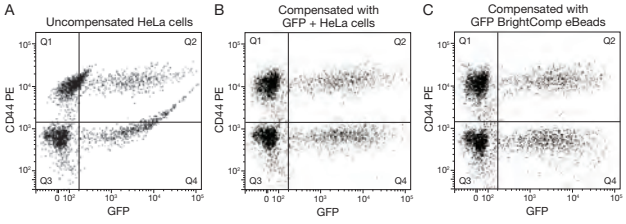

GFP compensation in flow cytometry. Samples either **(A)** were left uncompensated or were compensated with **(B)** GFP-expressing HeLa cells or **(C)** Invitrogen™ GFP BrightComp eBeads™ Compensation Beads (Cat. No. A10514). Both methods of GFP compensation produced the same degree of correction for spectral overlap.

Product	Quantity	Cat. No.
GFP BrightComp eBeads™ Compensation Bead Kit	25 tests	A10514

Measure hypoxia in live cells with Image-iT hypoxia reagents

Invitrogen™ Image-iT™ Red Hypoxia Reagent, and the recently introduced Invitrogen™ Image-iT™ Green Hypoxia Reagent, are cell-permeant fluorogenic compounds for measuring hypoxia in live cells. These reagents are nonfluorescent in an environment with normal oxygen concentrations (approximately 20%), and become increasingly fluorescent as oxygen levels are decreased, making them ideal tools for detecting hypoxic conditions in tumor cells, 3D cultures, spheroids, neurons, and other cells and tissues used in hypoxia research.

The Image-iT Red Hypoxia Reagent exhibits a fluorescent signal that responds to the current oxygen concentration, increasing as oxygen levels decrease and decreasing as oxygen levels increase; thus, it can be used as a real-time oxygen detector. In contrast, the fluorescence of the Image-iT Green Hypoxia Reagent increases as oxygen levels decrease but does not decrease if oxygen levels return to normal. This characteristic, combined with its ability to be fixed with minimal loss of fluorescent signal, allows it to be used as an endpoint hypoxia probe. Both reagents are extremely easy to use: just add to cell culture medium and image cells. For more information on the Image-iT hypoxia reagents, go to **thermofisher.com/hypoxia**.

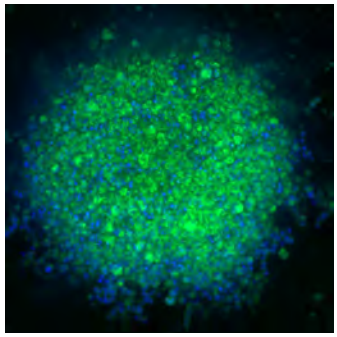

Detection of hypoxia in a spheroid. An A549 spheroid was stained with 5 µM Invitrogen™ Image-iT™ Green Hypoxia Reagent (green, Cat. No. I14834) and Invitrogen™ NucBlue™ Live ReadyProbes™ Reagent (blue, Cat. No. R37605), and then imaged on a Thermo Scientific™ CellInsight™ CX7 LZR High-Content Analysis Platform using a 10x objective and confocal mode. The image is from a maximum intensity projection of 20 optical Z slices of 10 µm each.

Product	Quantity	Cat. No.
Image-iT™ Green Hypoxia Reagent	1 vial 5 vials	I14834 I14833
Image-iT™ Red Hypoxia Reagent	1 mg	H10498

New anti-FLAG resins now available

Thermo Scientific™ Pierce™ Anti-DYKDDDDK (Anti-FLAG) Magnetic Agarose and Affinity Resin are ideal for isolating multi-subunit protein complexes because the mild purification process tends not to disrupt subunit interactions. The FLAG tag (peptide sequence DYKDDDDK, 1,012 Da) is a short hydrophilic protein tag commonly used in conjunction with antibodies in protein pull-down assays to study protein–protein interactions; it can be fused to the C terminus or N terminus of a protein, inserted within a protein, or used in conjunction with other affinity tags such as 6xHis, HA, or c-Myc.

Pierce Anti-DYKDDDDK (Anti-FLAG) Magnetic Agarose and Affinity Resin have a binding capacity of ≥3 mg per milliliter of settled resin. DYKDDDDK-tagged proteins are easily eluted using 0.1 M glycine (pH 2.8). For gentle elution, Thermo Scientific™ Pierce™ 3x DYKDDDDK Peptide is available to competitively elute the immobilized protein. Learn more about these anti-FLAG resins at **thermofisher.com/tag-purification**.

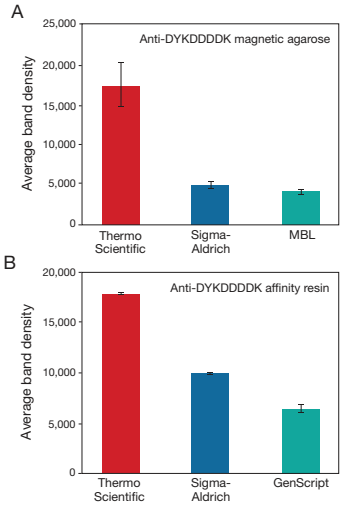

Comparison of results using anti-DYKDDDDK supports to purify DYKDDDDK-tagged SUMO protein. C- and N-terminal DYKDDDDK-tagged SUMO proteins were expressed in *E. coli* and purified using anti-DYKDDDDK supports from different suppliers. The tagged protein was competitively eluted with Thermo Fisher™ Pierce™ 3x DYKDDDDK Peptide and analyzed by SDS-PAGE and densitometry.

Product	Quantity	Cat. No.
Pierce™ Anti-DYKDDDDK Magnetic Agarose	1 mL 5 mL	A36797 A36798
Pierce™ Anti-DYKDDDDK Affinity Resin	1 mL 5 mL	A36801 A36803
Pierce™ 3x DYKDDDDK Peptide	5 mg	A36805

New protease inhibitor capsules for 500 mL volumes

Thermo Scientific™ Pierce™ Protease Inhibitor XL Capsules (EDTA-free) are ideal for reagent preparation prior to extracting proteins from tissue and cultured cells. They contain a broad-spectrum formulation of four protease inhibitors (AEBSF, bestatin, E-64, and pepstatin A) for better protection than that provided by phenylmethylsulfonyl fluoride (PMSF).

Each capsule is sufficient for 500 mL of solution. Simply open and empty the capsule into your reagent vessel, and watch the contents dissolve into a clear solution within minutes. This formulation is directly compatible with Thermo Scientific™ Pierce™ BCA Assays. The capsules are stable at 4°C with a minimum shelf life of one year. Find out more at thermofisher.com/inhibitorcocktails.

Product	Quantity	Cat. No.
Pierce™ Protease Inhibitor XL Capsules, EDTA-free	10 capsules	A37989

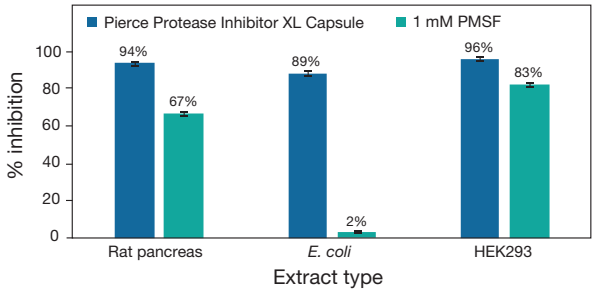

Performance comparison between Pierce Protease Inhibitor XL Capsule and phenylmethylsulfonyl fluoride (PMSF). Pancreatic extract (100 µL, 0.5 µg/µL), *E. coli* extract (100 µL, 0.5 µg/µL), or HEK293 extract (100 µL, 0.25 µg/µL) was incubated with a quenched fluorescent trypsin-cleavable substrate in the presence of Invitrogen™ Pierce™ Protease Inhibitor XL capsules or 1 mM PMSF. Reactions were incubated for 1 hr at 37°C, and fluorescence was determined at the appropriate emission. Percent protease inhibition is shown.

NeuCode amino acids enable higher multiplexing for SILAC

Stable isotope labeling with amino acids in cell culture (SILAC) is a powerful method for identifying and quantifying relative differential changes in complex protein samples. The SILAC method uses metabolic incorporation of heavy ^{13}C- or ^{15}N-labeled amino acids into proteins followed by mass spectrometry analysis for accelerated and comprehensive identification, characterization, and quantitation of proteins.

Thermo Scientific™ NeuCode™ amino acids augment the level of multiplexing achievable in metabolic labeling of proteins for mass spectrometry analysis, from 2-plex (heavy vs. light) to 4-plex. NeuCode metabolic labeling is similar to SILAC but differs in that the labeling only utilizes heavy amino acids. The increased multiplexing capability of NeuCode amino acids is possible through the use of mass defects from extra neutrons in the stable isotopes. These small mass differences may be resolved on high-resolution mass spectrometers. Learn more at thermofisher.com/silac.

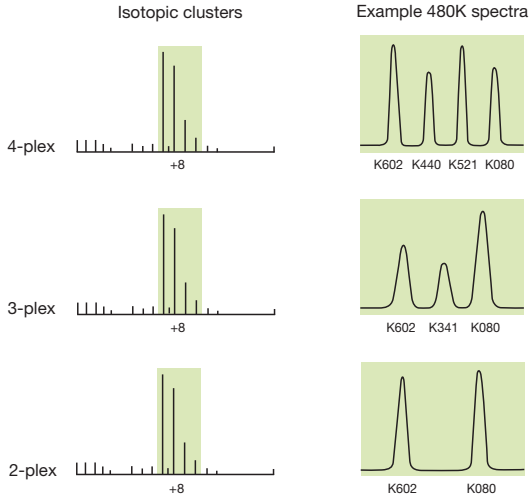

Different combinations of lysine isotopologs can be used to increase multiplexing from 2-plex to 4-plex at high resolution.

Product	Quantity	Cat. No.
NeuCode™ Lysine-080 (3,3,4,4,5,5,6,6-D_8 L-Lysine-2HCl)	25 mg	A36750
NeuCode™ Lysine-602 ($^{13}C_6$ $^{15}N_2$ L-Lysine-2HCl)	25 mg	A36751
NeuCode™ Lysine-440 (3,4,5,6-$^{13}C_4$, 5,5,6,6-D_4 L-Lysine-2HCl)	25 mg	A36752
NeuCode™ Lysine-521 (1,2,3,4,5-$^{13}C_5$, 6,6-D_2,^{15}N L-Lysine-2HCl)	25 mg	A36753
NeuCode™ Lysine-341 (3,4,5-$^{13}C_3$, 5,5,6,6-D_4,^{15}N L-Lysine-2HCl)	25 mg	A36851
NeuCode™ Lysine-202 ($^{13}C_2$ $^{15}N_2$ L-Lysine-2HCl)	25 mg	A36754
NeuCode™ Lysine 4-Plex Bundle (NeuCode™ Lysine-080, NeuCode™ Lysine-602, NeuCode™ Lysine-440, NeuCode™ Lysine-521)	1 bundle	A36755

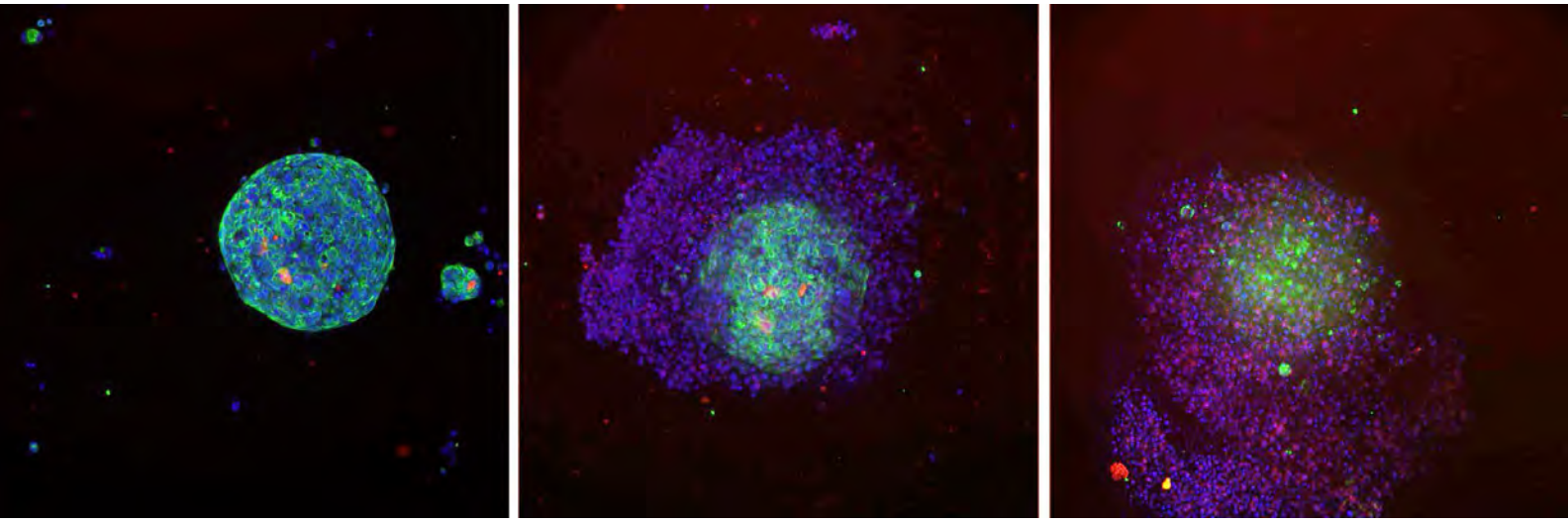

Immuno-oncology: Advances in basic research and translational medicine

With a focus on immune checkpoint inhibitors and T cell immunotherapy.

Developing methods for the prevention, diagnosis, and treatment of over 100 different types of cancer is the core objective in research laboratories around the world. In 2012, the International Agency for Research on Cancer reported 14.1 million new cancer cases and 8.2 million cancer deaths worldwide, and these numbers are expected to increase as a result of growing and aging global populations [1]. Although there have been improvements in surgery, radiation therapy, and chemotherapy treatments along with a decline in the rate of cancer deaths over the last few decades, metastatic disease is rarely completely controlled with conventional approaches. Moreover, debilitating side effects are frequently associated with radiation and chemotherapy.

Figure 1 (above). Chimeric antigen receptor (CAR) T cell invasion into cancer spheroids. See experimental details in Figure 7 caption.

According to the American Society of Clinical Oncology (ASCO), people living with cancer are benefiting from recent advances in cancer immunotherapy research—a field of study that began more than a century ago. The overarching goal of these novel treatment approaches is to enhance or enable anti-tumor immune responses, to overcome tumor evasion mechanisms, and to promote conditions that favor immune protection (Figure 1). Immunotherapy may offer distinct advantages over standard treatment modalities. For example, tumor-specific immune cells have the ability to migrate to areas of the body that are inaccessible by surgery. Cells of the immune system may also target microscopic disease and disseminated metastases. Furthermore, compared with radiation and chemotherapy, immunotherapy has been shown to act specifically against the tumor, thereby lowering the risk of damage to surrounding healthy tissue and minimizing side effects associated with standard cancer treatments. Nevertheless, severe toxicities may be associated with some particular immunotherapies [2].

Demonstrated promise of immunotherapies

Successes were realized in the past two decades with the development of novel cancer therapies known as immune checkpoint inhibitors (ICIs) [3]. ICIs are drugs (typically antibodies) that block either the immunosuppressive proteins on the surface of cancer cells or the T cell proteins that recognize them, thereby allowing T cells to mount an immune response. For example, with respect to certain solid tumors, administration of monoclonal antibodies (mAbs) that block T cell–expressed costimulatory receptors such PD-1 and CTLA-4 augment the cytolytic activity of $CD8^+$ T cells (killer T cells) within the tumor microenvironment (TME). Multiple studies have shown that these immune modulatory agents (Tables 1 and 2) increase overall survival in preclinical cancer models and are promising for treating human subjects with cancers of the skin, lung, bladder, or other organs. In-depth understanding of T cell biology has also supported advancement of cellular therapies, including T cell adoptive immunotherapies with engineered antigen receptors—approaches that epitomize the concept of personalized medicine.

Immune modulation of the tumor microenvironment

The TME is composed of a complex network of tumor cells and cells of the stroma, immune system, vasculature, and extracellular matrices (Figure 2). Although tumor-infiltrating immune cells are present in the TME, the immunosuppressive milieu must be overcome to achieve antigen recognition, T cell priming and activation, and the expansion of tumor antigen–specific cytotoxic T cells. In addition to various cytokines that drive or inhibit immune responses, Figure 2 lists several T cell co-receptors (or their ligands), including ICIs, that are rational drug targets for immunotherapy—some of which are targets of cancer therapy agents approved by →

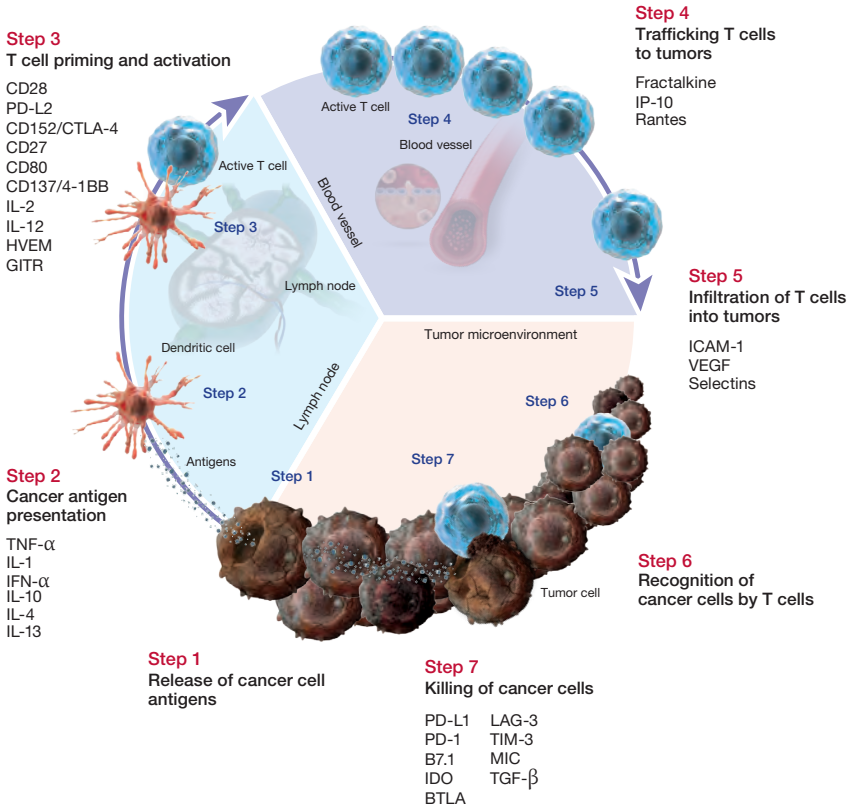

Figure 2. The multistep anti-tumor responses. The cancer immunity cycle involves the coordination of a myriad of checkpoint molecules and other cell-surface receptors, as well as soluble factors such as cytokines and chemokines. The process is initiated by the release of tumor-derived antigens (step 1). The engulfment of these antigens by dendritic cells and their subsequent presentation to T cells (steps 2 and 3) drive the immune response. Once activated, effector T cells acquire the ability to destroy target cells by specifically recognizing tumor peptide–MHC complexes displayed on the tumor cell surface (steps 4–7). Increasing levels of tumor antigens are then released, further driving the progression of the cycle. ICIs have been shown to augment the T cell–mediated tumor rejection.

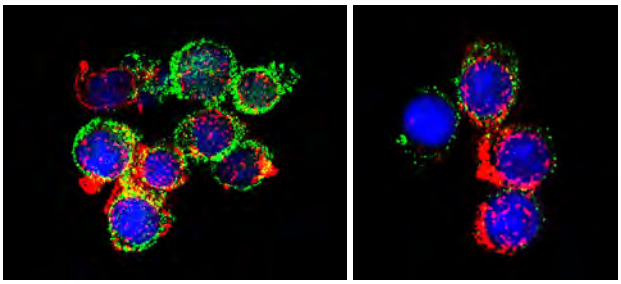

Figure 3. Immunofluorescence analysis of Jurkat cells using anti–CTLA-4 antibody. PMA-treated (left) and untreated (right) Jurkat cells were fixed and permeabilized for detection of endogenous CTLA-4 using Invitrogen™ ABfinity™ anti–CTLA-4 recombinant rabbit monoclonal antibody (clone 11H7L17, Cat. No. 702534) in conjunction with Invitrogen™ Superclonal™ goat anti–rabbit IgG (H+L) secondary antibody, Alexa Fluor™ 488 conjugate (Cat. No. A27034). Cell-surface localization of CTLA-4 protein is represented by the green signal. Nuclei (blue) were counterstained with Invitrogen™ SlowFade™ Gold Antifade Mountant with DAPI (Cat. No. S36938); cytoskeletal F-actin (red) was labeled with rhodamine phalloidin (Cat. No. R415). Compared with the untreated cells in the right panel, cells treated with PMA (5 ng/mL, 48 hr; left panel) show an upregulation of CTLA-4 protein. The images were captured at 60x magnification on a Nikon™ Eclipse™ Ti-E Inverted Microscope.

the US Food and Drug Administration (FDA). Table 1 provides details on the first-generation ICIs that are currently approved for indications in cancer. Figure 3 shows an example of Jurkat cells stained with a research antibody that recognizes the human CTLA-4 receptor.

Methods for identifying immune cells in TME, blood, and culture

Immune cell subsets within the TME include, but are not limited to, dendritic cells (DCs), natural killer (NK) cells, B cells, and T cells (including $CD4^+$ T helper and regulatory subsets, $CD8^+$ cytotoxic T cells with the potential to directly eradicate tumor cells, and other T cell subsets). The TME also harbors cells of the myeloid lineages, which may have both tumor-suppressive and tumor-promoting properties. The ability to isolate, characterize, and modulate cells that populate the TME is directly linked to advances in basic biomedical research and translational medicine. To learn more about leukocyte subsets and flow cytometry, access the T cell proliferation and stimulation ecourse at **thermofisher.com/elearningcourses.**

Flow cytometry. Figure 4 illustrates how tumor-infiltrating lymphocytes (TIL) isolated from mice treated with or without anti–mouse CTLA-4 monoclonal antibody (mAb) may be evaluated *ex vivo* by multicolor flow cytometry—a powerful technology for phenotyping heterogeneous cell populations [4]. In this study by Draper et al., splenocytes were isolated from mice after administration of a total of 5 doses of anti–CTLA-4 mAb at 10 mg per kilogram of body weight, delivered 3 times weekly. Shown is the gating strategy used to define B cell, $CD4^+$ helper T cell, Treg, $CD8^+$ T cell, and NK cell populations. Cell proliferation was monitored by detecting the carboxyfluorescein succinimidyl ester (CFSE)–labeled leukocyte populations of interest. Use of this representative antibody staining protocol, CSFE labeling method, and gating strategy provides an effective way to evaluate the effects of ICI treatment in mouse tumor models. To learn more about the Invitrogen™ Attune™ NxT Flow Cytometer, flow cytometry reagents, and antibodies, go to **thermofisher.com/flowcytometry**.

Immunoassays for soluble proteins. In addition to implementing flow cytometry methods, immunophenotyping may be accomplished

Table 1. Approved T cell co-receptor–associated targets of cancer immunotherapy.

Agent	Target	Indication (initial FDA approval year)	Pivotal clinical trial reference
Ipilimumab	CTLA-4	Melanoma (2011) [1]	Hodi FS, O'Day SJ, McDermott DE et al. (2010) *N Engl J Med* 363:711–723.
Pembrolizumab	PD-1	Melanoma, NSCLC, HNSCC, cHL (2014) [2]	Hamid O, Robert C, Daud A et al. (2013) *N Engl J Med* 369:134–144.
Nivolumab	PD-1	Melanoma, NSCLC, RCC, cHL, SCCHN, UC, dMMR solid cancers, CRC, HCC (2014) [3]	Weber JS, D'Angelo SP, Minor D et al. (2015) *Lancet Oncol* 16:375–384.
Atezolizumab	PD-L1	Bladder, NSCLC (2016) [4]	Rosenberg JE, Hoffman-Censits J, Powles T et al. (2016) *Lancet* 387:1909–1920.
Avelumab	PD-L1	MCC, bladder (2017) [5]	Kaufman HL, Russell, J, Hamid O et al. (2016) *Lancet Oncol* 17:1374–1385.
Durvalumab	PD-L1	Bladder (2017) [6]	Antonia SJ, Vilegas A, Daniel D et al. (2017) *N Engl J Med* 377:1919–1929.

Colorectal cancer (CRC); classical Hodgkin lymphoma (cHL); hepatocellular carcinoma (HCC); Merkel cell carcinoma (MCC); mismatch repair deficient (dMMR); non-small cell lung cancer (NSCLC); renal cell carcinoma (RCC); squamous cell carcinoma of the head and neck (SCCHN). 1. Yervoy prescribing information (2015) Bristol-Myers Squibb Company. Accessed 15 January 2018. **accessdata.fda.gov/drugsatfda_docs/label/2015/125377s073lbl.pdf**. 2. Keytruda prescribing information (2014) Merck & Co., Inc. Accessed 15 January 2018. **merck.com/product/usa/pi_circulars/k/keytruda/keytruda_pi.pdf**. 3. Opdivo prescribing information (2018) Bristol-Myers Squibb Company. Accessed 15 January 2018. **packageinserts.bms.com/pi/pi_opdivo.pdf**. 4. Tecentriq prescribing information (2017) Genentech, Inc. Accessed 15 January 2018. **gene.com/download/pdf/tecentriq_prescribing.pdf**. 5. Bavencio prescribing information (2017) EMD Serono, Inc. **emdserono.com/ms.country.us/en/images/Bavencio_PI_tcm115_161084.pdf**. 6. Imfinzi prescribing information (2017) AstraZeneca Pharmaceuticals LP. Accessed 15 January 2018. **azpicentral.com/imfinzi/imfinzi.pdf**.

using sophisticated immunoassays that measure soluble proteins. The Invitrogen™ Immuno-oncology Checkpoint 14-Plex Human ProcartaPlex™ Panel 1 is a novel immunoassay that utilizes Luminex® xMAP® technology for the multiplex detection of the soluble immune checkpoint protein analytes displayed in Figure 5. An increasing number of studies suggest that these soluble proteins have the potential to function as decoy receptors or as immune adjuvants that may interfere with the efficacy of checkpoint modulator drug candidates. Additionally, evaluating soluble immune checkpoint protein biomarkers in sera or plasma of cancer patients may offer a minimally invasive method for correlating ICI treatment efficacy with analyte concentrations or for enabling identification of individuals that may or may not respond to a given ICI therapy.

This concept was first demonstrated in a study that reported a positive correlation between elevated serum levels of soluble CTLA-4 and clinical outcome benefit in patients treated with ipilimumab [5]. This ProcartaPlex panel is suitable for use with the Luminex 200™, FLEXMAP 3D®, and MAGPIX® systems, and data for multiple analytes may be obtained from small sample volumes (25 µL for serum or plasma samples, 50 µL for cell culture supernatant). Similar to conventional immunoassays, antigen quantitation is accomplished using a fluorescently labeled secondary antibody, and signal intensity is proportional to the concentration of protein detected. Importantly, this multiplex assay produces results that overlap with those obtained with singleplex plate-based enzyme-linked immunosorbent assays (ELISA). Visit **thermofisher.com/luminex** to learn more about multiplex assays using Luminex technology and the ProcartaPlex →

Table 2. Representative examples of investigational ICI agents.

Agent	Target	Development stage
rHIGM12B7	PD-L2	Phase I
Tremelimumab	CTLA-4	Phase I–III
IMP321, BMS-986016	LAG-3	Phase I–II; Phase I–II
TSR-022	TIM-3	Phase I
PBF-509	A2aR	Phase I

To learn more about ICI antibodies for flow cytometry, IHC, and functional bioassays, see the related article in *BioProbes 75 Journal of Cell Biology Applications* (May 2017) titled "Harness immune checkpoints to combat tumors" at thermofisher.com/bp75.

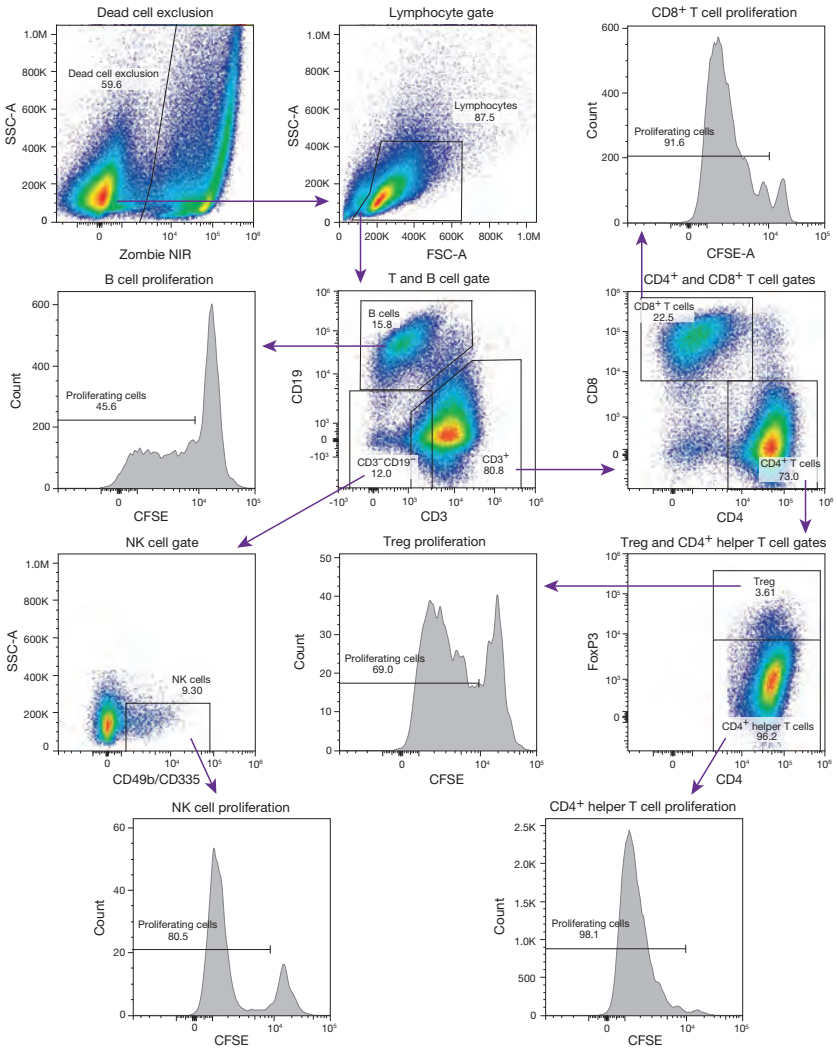

Figure 4. Profile of splenocytes (derived from a Balb/c syngenic CT26 colorectal tumor model) stimulated with anti-CD3 antibody. Tumor-naive and tumor-bearing mice were left untreated or administered anti–mouse CTLA-4 antibody. Subsequently, splenocytes were harvested, preloaded with carboxyfluorescein succinimidyl ester (CFSE), stimulated, stained, and analyzed on the Invitrogen™ Attune™ NxT Flow Cytometer. All procedures were performed according to the investigator's protocols. Data used with permission from David Draper and Alden Wong, MI Bioresearch, Ann Arbor, Michigan, USA.

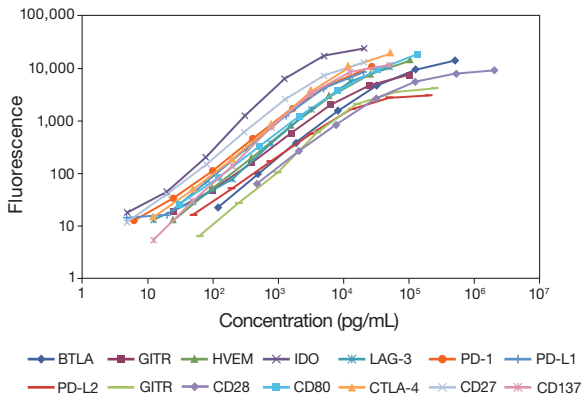

Figure 5. Analysis of 14 soluble protein biomarkers in a single sample using a ProcartaPlex immunoassay. Standard curves are shown for the Invitrogen™ Immuno-oncology Checkpoint 14-Plex Human ProcartaPlex™ Panel 1 (Cat. No. EPX14A-15803-901).

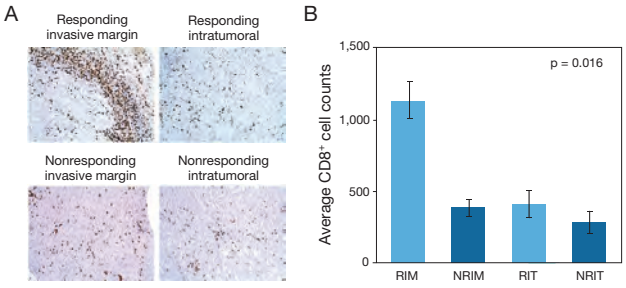

Figure 6. Tumors responding to treatment show increased T cell infiltration prior to therapy. (A) Representative CD8+ immunohistochemical (IHC) staining of the invasive tumor margin and intratumoral region in pretreatment metastatic melanoma tumors (responding N = 4, nonresponding N = 4). Tumor compartments were assessed by a dermatopathologist. **(B)** Average CD8+ cell counts for responding and nonresponding tumor compartments. T cell counts were produced by averaging the counts of 10 randomly selected fields using a 20x objective for each tumor compartment (10 invasive margin; 10 intratumoral). RIM = responding invasive margin; NRIM = nonresponding invasive margin; RIT = responding intratumoral; NRIT = nonresponding intratumoral. Reprinted with permission from Shields B, Mahmoud F, Taylor EM et al. (2017) *Sci Rep* 7:807, and under the Creative Commons Attribution 4.0 International License (**creativecommons.org/licenses/by/4.0/**).

immuno-oncology checkpoint panels in particular (Figure 5). Visit **thermofisher.com/procartaplex-immunocheckpoints** to read the application note "Detection of soluble isoforms of immuno-oncology checkpoint markers".

Cell imaging analysis. Both cell-imaging microscopes and high-content analysis (HCA) instruments are particularly robust tools that enable researchers to assess the structure, localization, and endogenous expression levels of proteins of interest and other cell characteristics. Invitrogen™ EVOS™ Imaging Systems may be employed for transmitted-light imaging as well as colorimetric and fluorescence imaging for qualitative assessments; quantitative information about protein relocalization or organelle function can be obtained after importing images into data analysis software such as ImageJ. Figure 6 shows an example of data produced using the EVOS FL Auto Imaging System. Compared with observations in nonresponding metastatic melanoma patients treated with anti–CTLA-4 or anti–PD-1 mAbs, this immunohistochemical analysis indicates that, prior to treatment, statistically significant numbers of CD8+ T cells accumulated in the invasive margin of tumors from patients that responded to ICI therapy [6]. Learn more about EVOS Imaging Systems at **thermofisher.com/evos**.

High-content imaging and analysis. HCA technology combines high-resolution microscopy and automated image capture with multiparametric acquisition and data analysis to provide precise quantitative analysis of individual cells in a large and potentially heterogeneous cell population. With the aid of molecular tools such as fluorescent dyes, chemical probes, and targeted antibodies, a wide range of cell events and features can be quantitated, including but not limited to nuclei and DNA counts, nuclear and whole-cell morphology, and cytoskeletal organization, as well as cell motility, migration, and invasion [7]. In addition, these features can be quantitated over time to evaluate temporal and spatial relationships between multiple cellular targets in intact cells. An important advantage of HCA is the ability to perform multiple independent measurements simultaneously, and cell-based HCA assays are increasingly being used to monitor mechanisms critical in immuno-oncology research [8]. To produce the data presented in Figure 7, a Thermo Scientific™ CellInsight™ CX7 High-Content Analysis Platform was used to visualize effector T cell–mediated lysis of HCC827 cancer spheroids. Compared with the negative control conditions shown in the left panel, increasing the effector:target ratio resulted in a greater degree of target cell lysis, as seen in the right panel [9]. To learn more about Thermo Scientific™ high-content imaging and analysis instruments and reagents, go to **thermofisher.com/hca**.

Alternative ICI T cell targets and additional strategies for cancer immunotherapy

The ICIs listed in Table 1 may become first-line therapies for certain advanced cancers; however, these treatments—either alone or in combination with other immunotherapy or chemotherapy agents—have been successful in a minority of patients. Table 2 provides a nonexhaustive summary of ICI drug candidates for the treatment of various solid and

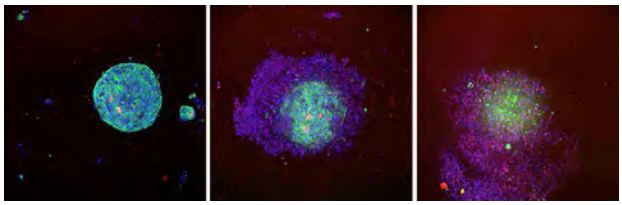

Figure 7. Chimeric antigen receptor (CAR) T cell invasion into cancer spheroids. HCC827 spheroids were formed using spheroid microplates for 48 hr. Then, 24 hr after the addition of EGFR scFv-CD28-CD3ε CAR T cells (ProMab Biotechnologies), spheroids were immunostained for cytokeratin-7 (green) and CD3ε (red), and counterstained with Hoechst™ dye (blue). As the effector-to-target ratio is increased from 10:1 (middle panel) to 40:1 (right panel), invasion of the CAR T cells into the HCC827 tumor spheroid and subsequent tumor cell lysis are visible. Images were obtained on the Thermo Scientific™ CellInsight™ CX7 High-Content Analysis Platform in confocal mode with a 10x objective, and used with permission from Corning Inc.

hematological tumors, administered alone or as combinatorial drug therapies with other ICIs or chemotherapy [10,11].

Beyond developing biotherapeutic antibodies that target immune checkpoint pathways, over the past few decades researchers have harnessed the power of adoptive cell therapies (ACT). For example, in adoptive T cell transfer, a patient's T cells are extracted, genetically modified to recognize the cancer cells, cultured *in vitro*, and then reintroduced into the patient. In 1988, autologous T cell adoptive transfer of *ex vivo* expanded cells was used with relative success to treat patients with metastatic melanoma resistant to conventional therapies, and incremental improvements in efficacy have emerged over time [12]. More recently, investigators have realized gains with the development of chimeric antigen receptor (CAR) T cell therapy for treating certain forms of cancer (Figure 7). In 2017, two CAR T cell therapies were approved by the FDA, opening the door for a new generation of ACTs.

Another emerging field inspiring great interest is immuno-metabolism, which explores intracellular metabolic pathways in immune cells. Among several focus areas, researchers are seeking to understand how drugs may selectively target metabolic pathways that govern T cell function and how alterations in T cell metabolism may potentially boost tumor rejection *in vivo* [13,14].

Download the Immuno-oncology Guide

To learn more about technologies that enable immuno-oncology research, download the Immuno-oncology Flow Cytometry Guide (at **thermofisher.com/flow-io**), which provides detailed information about workflows for flow cytometry, biomarker profiling, and cell imaging, and reviews several central aspects of cancer research. ■

References

1. "Global Cancer Facts & Figures" American Cancer Society. cancer.org/research/cancer-facts-statistics/global.html
2. Dimberu PM, Leonhardt RM (2011) *Yale J Biol Med* 84:371–380.
3. "Immunotherapy 2.0 named Advance of the Year in ASCO's 12th Annual Cancer Progress Report" ASCO, 15 Apr 2017. asco.org/about-asco/press-center/news-releases/immunotherapy-20-named-advance-year-asco%E2%80%99s-12th-annual-cancer
4. Draper D, Wong A, Saims D et al. (2017) "Abstract 5624: Characterization of proliferation in multiple lymphocyte subsets in the CT26 carcinoma model by multi-color flow cytometry". Presented at: American Association for Cancer Research Annual Meeting 2017; April 1–5, 2017; Washington, D.C., USA.
5. Weber JS (2017) "What has the checkpoint inhibitor experience in melanoma taught us about immunotherapy for other cancers?" ASCO Daily News. am.asco.org/what-has-checkpoint-inhibitor-experience-melanoma-taught-us-about-immunotherapy-other-cancers
6. Shields BD, Mahmoud F, Taylor EM et al. (2017) *Sci Rep* 7:807.
7. Fraietta I, Gasparri F (2016) *Expert Opin Drug Discov* 11:501–514.
8. Li L, Zhou Q, Voss TC et al. (2016) *Methods* 96:97–102.
9. Gitschier H (2017) Advanced Models for 3D Screening: Immune Oncology Applications. AACR April 2017. Accessed 8 January 2018. corning.com/media/worldwide/cls/documents/Advanced-Models-for-3D-Screening-Immune-Oncology-Applications.pdf
10. Tchekmedyian N, Gray JE, Creelan BC et al. (2015) *Oncology (Williston Park)* 29:990–1002.
11. clinicaltrials.gov
12. Rosenberg SA, Restifo NP, Yang JC et al. (2008) *Nat Rev Cancer* 8:299–308.
13. O'Neill LA, Kishton RJ, Rathmell J (2016) *Nat Rev Immunol* 16:553–565.
14. Dugnani E, Pasquale V, Bordignon C et al. (2017) *Cancer Lett* 28:12–18.

Product	Quantity	Cat. No.
Selected antibodies and immunoassays		
ADORA2A Polyclonal Antibody	100 µL	PA1-042
CD223 (LAG-3) Monoclonal Antibody (3DS223H), FITC	100 tests	11-2239-42
CD273 (PD-L2, B7-DC) Monoclonal Antibody (122), FITC	100 µg	11-9972-82
CD274 (PD-L1, B7-H1) Monoclonal Antibody (MIH5), PE	100 µg	12-5982-82
CD274 (PD-L1, B7-H1) Monoclonal Antibody (MIH1), PE	100 tests	12-5983-42
CD279 (PD-1) Monoclonal Antibody (MIH4), FITC	25 tests	11-9969-41
CD279 (PD-1) Monoclonal Antibody (J116)	100 µg	14-9989-82
CD366 (TIM-3) Monoclonal Antibody (F38-2E2), Super Bright 702	100 tests	67-3109-42
CTLA-4 ABfinity™ Rabbit Monoclonal Antibody (11H7L17)	100 µg	702534
Immuno-oncology Checkpoint 14-Plex Human ProcartaPlex™ Panel 1	96 tests	EPX14A-15803-901
Immuno-oncology Checkpoint 14-Plex Human ProcartaPlex™ Panel 2	96 tests	EPX140-15815-901
PD-L1 Polyclonal Antibody	100 µg	PA5-20343
Fluorescence instrumentation		
Attune™ NxT Flow Cytometer, blue/violet6	1 each	A29002
Attune™ NxT Flow Cytometer, blue/red/violet6	1 each	A29003
Attune™ NxT Flow Cytometer, blue/red/violet6/yellow	1 each	A29004
Attune™ NxT Violet Laser Upgrade Kit	1 kit	100022777
CellInsight™ CX7 High-Content Analysis Platform	1 each	CX7A1110
EVOS™ FL Auto 2 Imaging System	1 system	AMAFD2000

Antibodies for stem cell research

Using stem cell differentiation models to verify antibody specificity.

Due to their regenerative capabilities, stem cells have tremendous potential for use in cell therapy for degenerative disorders, including Alzheimer's and Parkinson's diseases, as well as for disease modeling, drug screening, and developmental biology research [1]. Stem cells are undifferentiated cells that have the capacity both to self-renew through mitosis and to differentiate into specialized cell types such as neuronal, liver, or muscle cells. Characterization of stem cells using antibodies is a critical step in stem cell research and relies on highly specific antibodies that perform well in the particular cell analysis platform.

Use of stem cell differentiation models for antibody characterization

As vital reagents for stem cell research, antibodies that recognize specific stem cell biomarkers can be used for cell imaging, cell sorting, immunoassays, and other relevant applications. At the same time, stem cells differentiated along various lineages can be a powerful tool for determining the cell and tissue specificity of antibodies. In cases such as specialized neurons, where it is especially difficult to obtain the right cell model, neural stem cells differentiated into the required mature neurons can be a standardized way to validate neuron-specific antibodies. Here we highlight several examples of our use of stem cell differentiation models to evaluate antibody specificity.

Antibodies for neuronal markers

Nestin and SOX2 are neuronal progenitor markers expressed on neuronal stem cells (NSCs). To confirm the specificity of our anti-nestin and anti-SOX2 antibodies, we tested them with human neural stem cells (NSCs) differentiated from H9-derived embryonic stem cells (ESCs) and observed the expected expression patterns (Figures 1A and 1B). Similarly, antibodies against mature neuronal markers MAP2 and β-III tubulin (Figures 1C and 1D) and GFAP (Figure 1E) were tested with differentiated neurons derived using Gibco™ StemPro™ NSC SFM (Neural Stem Cell Serum-Free Medium).

ABfinity antibodies for developmental markers

We are also continuing to develop Invitrogen™ ABfinity™ recombinant antibodies for important developmental transcription factors. ABfinity antibodies are highly specific recombinant monoclonal antibodies developed by immunizing animals with the antigen, screening antibodies for desired functionality, and then cloning the immunogen-specific antibody genes into high-expression vectors. The antibodies are produced on a large scale by expressing them in mammalian cells, and then highly purified with protein A. These recombinant antibodies can be used just like traditional IgG antibodies but are designed to provide very consistent results from lot to lot, saving time and money because assays do not require revalidation.

SOX9 is a member of the SOX family of developmental transcription factors that are related to the Y-chromosome sex-determining factor

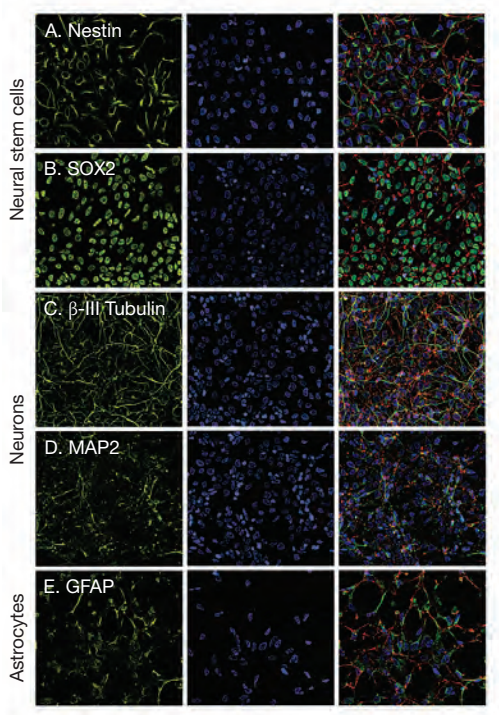

Figure 1. Characterization of neural antibodies using differentiated embryonic stem cells. Human neural stem cells (NSCs) differentiated from H9-derived embryonic stem cells using Gibco™ PSC Neural Induction Medium (Cat. No. A1647801) were used to characterize antibodies against neural progenitor markers **(A)** nestin (Cat. No. MA1110) and **(B)** SOX2 (Cat. No. MA1014). Differentiated neurons derived from NSCs using Gibco™ StemPro™ NSC SFM (Cat. No. A1050901) were used to characterize antibodies against mature neuronal markers **(C)** MAP2 (Cat. No. 131500) and **(D)** β-III tubulin (Cat. No. 322600); an antibody against **(E)** GFAP (Cat. No. MA512023) was characterized using differentiated astrocytes. Primary monoclonal antibodies were detected with Invitrogen™ Alexa Fluor™ 488 goat anti–mouse IgG secondary antibody (green, left column; Cat. No. A28175), nuclei were stained with DAPI (blue, middle column; Cat. No. D1306), and F-actin was labeled with rhodamine phalloidin (red, Cat. No. R415); right column shows composite images. Appropriate negative controls (MAP2 in neural stem cells and astrocytes, and nestin in neurons) were used to determine specificity (data not shown).

SRY. SOX9, which functions in the development of multiple organs, was recently reported to be involved in the early differentiation of ESCs into three germ layers [2]. The specificity of an ABfinity anti-SOX9 antibody was evaluated using the Gibco™ Human Episomal iPSC Line and the embryoid bodies (EBs) derived from them (Figure 2). As expected, nuclear localization of SOX9 was observed only in the EBs, which are predominantly composed of progenitors of all three germ layers, whereas expression was completely absent in the undifferentiated cells.

RUNX2 is a critical regulator of osteogenic development and plays an essential role in the specification of osteogenic lineage by inducing the expression of extracellular matrix proteins during maturation. Its expression during osteoblast differentiation is temporally controlled, peaking at day 7 and decreasing to undetectable levels by day 14 [3-5]. Human bone marrow–derived mesenchymal stem cells (MSCs) were differentiated to osteocytes using the Gibco™ StemPro™ Osteogenesis Differentiation Kit, and the specificity of an ABfinity anti-RUNX2 antibody was evaluated on cells throughout this differentiation process, from day 0 to day 14 (Figure 3). As expected, RUNX2 expression was absent in undifferentiated MSCs, specifically localized to the early osteoblast at day 7, and then undetectable in the mature osteoblast at day 14.

Find your stem cell antibody

Advances in the field of stem cell therapy are critically dependent on the availability of highly specific antibodies that have been validated in biologically relevant model systems; find out more about our stringent antibody validation* criteria at **thermofisher.com/antibodyvalidation**. No matter which detection platform you use—flow cytometry, immunocytochemistry, western blot, or ELISA—our collection of over 51,000 Invitrogen™ antibodies provides you with tools compatible with your experimental design. Select the right antibodies for your stem cell targets at **thermofisher.com/antibodiesbp77**. ■

*The use or any variation of the word "validation" refers only to research-use antibodies that were subject to functional testing to confirm that the antibody can be used with the research techniques indicated. It does not ensure that the product or products were validated for clinical or diagnostic uses.

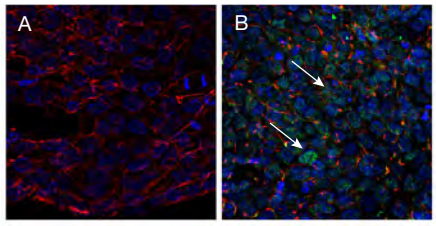

Figure 2. Acceleration by SOX9 of the differentiation of pluripotent stem cells to progenitors of all three lineages. Cells from the Gibco™ Human Episomal iPSC Line (Cat. No. A18945) labeled with anti-SOX9 antibody (Cat. No. 702016) and Invitrogen™ Alexa Fluor™ 488 goat anti–rabbit IgG secondary antibody (green, Cat. No. A27034) revealed that SOX9 is **(A)** absent in the human episomal iPS colony but **(B)** present in embryoid bodies (EBs), which are derived from the iPSC line and have progenitors of all three lineages (arrows). Nuclei were stained with DAPI (blue, Cat. No. D1306); F-actin was labeled with rhodamine phalloidin (red, Cat. No. R415).

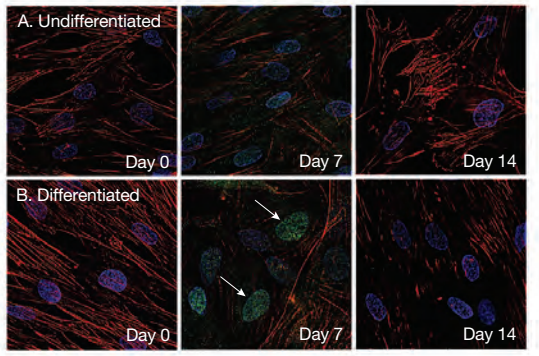

Figure 3. Activation by RUNX2 of osteoblast differentiation in human bone marrow–derived mesenchymal stem cells. Temporal RUNX2 expression at day 0, 7, and 14 in **(A)** undifferentiated human bone marrow–derived mesenchymal cells and **(B)** those subjected to osteoblast differentiation using the Gibco™ StemPro™ Osteogenesis Differentiation Kit (Cat. No. A1007201), as revealed by immunostaining with anti-RUNX2 antibody (Cat. No. 711519) and Invitrogen™ Alexa Fluor™ 488 goat anti–rabbit IgG secondary antibody (green, Cat. No. A27034) (arrows). Nuclei were stained with DAPI (blue, Cat. No. D1306); F-actin was labeled with rhodamine phalloidin (red, Cat. No. R415).

Product	Quantity	Cat. No.
Cells and media		
Human Episomal iPSC Line	1 x 10^6 cells	A18945
PCS Neural Induction Medium	500 mL	A1647801
StemPro™ Neural Stem Cells	1 x 10^6 cells	A15654
StemPro™ NSC SFM	1 kit	A1050901
StemPro™ Osteogenesis Differentiation Kit	1 kit	A1007201
Selected stem cell antibodies		
GFAP Monoclonal Antibody (ASTRO6)	500 µL	MA512023
MAP2 Monoclonal Antibody (M13)	100 µg	131500
Nestin Monoclonal Antibody (10C2)	100 µg	MA1110
RUNX2 ABfinity™ Rabbit Oligoclonal Antibody (6HCLC)	100 µg	711519
SOX2 Monoclonal Antibody (20G5)	100 µg	MA1014
SOX9 ABfinity™ Rabbit Monoclonal Antibody (7H13L8)	100 µg	702016
β-III Tubulin Monoclonal Antibody (2 28 33)	100 µg	322600

References

1. Wu J, Izpisua Belmonte JC (2016) *Cell* 165:1572–1585.
2. D'Aiuto L, Zhi Y, Kumar Das D et al. (2014) *Organogenesis* 10:365–377.
3. Komori T (2010) *Cell Tissue Res* 339:189–195.
4. Maruyama Z, Yoshida CA, Furuichi T et al. (2007) *Dev Dyn* 236:1876–1890.
5. Sudhakar S, Li Y, Katz MS et al. (2001) *Biochem Biophys Res Commun* 289:616–622.

Flow cytometry assay for simultaneous detection of HIV RNA and Gag protein

Single-cell characterization of viral translation-competent reservoirs in HIV-infected individuals.

Baxter AE, Niessl J, Fromentin R et al. (2016) *Cell Host Microbe* 20:368–380.

Dramatic advances in antiretroviral therapy (ART) have enabled the currently 71 million HIV-infected individuals worldwide to lead relatively normal lives, transforming HIV infection into a chronic but manageable disease. ART, however, mandates lifelong treatment, with interruption leading to immediate viral rebound and disease progression. Recent years have seen a push for HIV curative initiatives to relieve infected individuals of the multifaceted burdens of prolonged therapy. These strategies have been hampered by the fact that HIV establishes latent reservoirs in predominantly transcriptionally silent T cells that are impervious to currently available ART.

Studies suggest that a feasible approach to achieving a functional cure for HIV might entail a "shock and kill" tactic: using latency-reversing agents (LRA) to reactivate HIV reservoirs while simultaneously improving the host immune system to kill cells with reactivated virus [1]. A major hurdle in this approach has been establishing robust, high-throughput assays to identify HIV reservoirs or cells harboring viral RNA following LRA administration. The current gold standard for identifying HIV reservoirs capable of producing infectious virions is the quantitative viral outgrowth assay (QVOA) [2]. Unfortunately, QVOA is a time-consuming, labor-intensive, and costly method, impeding its widespread adaptation. Furthermore, the QVOA underestimates HIV reservoirs and, most importantly, offers no pertinent immunophenotypic information about the cells with reactivated HIV. Other methods include PCR-based assays such as droplet digital PCR (ddPCR) [3] and the Tat/rev-induced limiting dilution assay (TILDA) [4].

Multiple studies have identified HIV RNA as a potential biomarker of HIV reservoirs and an indicator of latency reversal during the "shock and kill" assays. A step toward identifying and optimizing HIV curative measures would be provided by a single-cell assay permitting robust HIV RNA detection and multiparametric characterization of infected cells expressing reactivated HIV RNA.

Baxter and colleagues have recently reported their use of the Invitrogen™ PrimeFlow™ RNA Assay (Figure 1) to detect viral translation–competent reservoirs in HIV-infected individuals [5]. The PrimeFlow RNA assay is a flow cytometry–based *in situ* hybridization assay that combines sensitive branched DNA (bDNA) amplification with single-cell resolution. Moreover, the PrimeFlow RNA assay is compatible with simultaneous immunophenotyping for cell-surface and intracellular proteins.

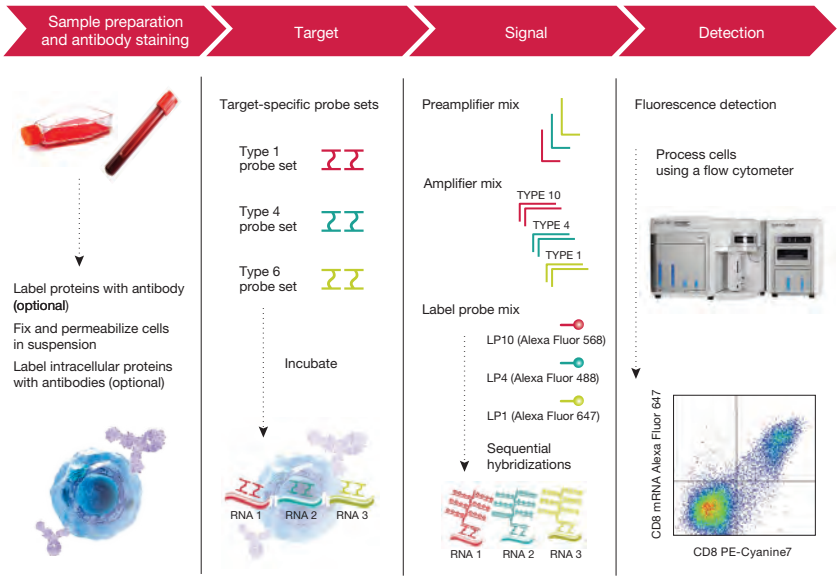

Figure 1. The PrimeFlow RNA Assay workflow. The workflow for the Invitrogen™ PrimeFlow™ RNA Assay Kit (Cat. No. 88-18005-204) starts with optional antibody labeling of cell-surface proteins followed by fixation, permeabilization, and optional antibody labeling of intracellular proteins. Next, the fixed and permeabilized cells are hybridized with RNA-specific target probes; up to 4 different RNA targets can be detected in a single experiment. This hybridization is then detected after branched DNA (bDNA) signal amplification using preamplifiers, amplifiers, and label probes, which comprise oligonucleotides conjugated to highly fluorescent Alexa Fluor™ 488, Alexa Fluor™ 568, Alexa Fluor™ 647, or Alexa Fluor™ 750 dyes. Labeled cells are analyzed on a standard flow cytometer.

Simultaneous HIV RNA and protein detection in T cells

In their recent publication, Baxter et al. describe the detection of CD4 T cells expressing HIV RNA (using probe sets against both the *GAG* and *POL* genes) and Gag protein (using anti-Gag antibody). They report that, after culturing CD4 T cells from untreated HIV-infected individuals (UNT) *in vitro* for 7–10 days, they could readily detect CD4 T cells positive for both HIV RNA and protein ($HIV^{RNA+/Gag+}$); after addition of antiretrovirals to this T cell culture (UNT + ARVs), $HIV^{RNA+/Gag+}$ T cells were undetectable.

They also examined CD4 T cells from untreated HIV-infected individuals (UNT) and ART-treated HIV-infected individuals (Tx) after stimulation with LRAs *in vitro*. After reservoir reactivation using PMA/ionomycin or a protein kinase C (PKC) agonist such as bryostatin and ingenol, translation-competent virus could be detected using the PrimeFlow RNA assay. In addition, the estimated reservoir size in the $HIV^{RNA+/Gag+}$ T cells correlated well with the size of reservoirs measured by orthogonal assays.

The PrimeFlow RNA assay is compatible with immunophenotyping, allowing these researchers to further characterize the T cells expressing reactivated virus. The central memory T cell (T_{CM}) subset had previously been identified as the predominant harbor of HIV reservoirs in infected individuals on ART. Using the PrimeFlow RNA assay, Baxter et al. confirmed that the T_{CM} subset in untreated infected individuals also harbored high levels of HIV, and that $HIV^{RNA+/Gag+}$ cells expressed the co-inhibitory markers PD-1, CTLA4, and TIGIT, contributing to T cell exhaustion, a hallmark of HIV infections.

Conclusions and potential for future HIV research

Baxter et al. showed that the PrimeFlow RNA assay could be used to assess the size of HIV reservoirs, to determine the efficacy of LRAs, and to establish the phenotype of cells expressing reactivated virus. Their conclusions complement those of other studies using the PrimeFlow RNA assay to study the kinetics of HIV transcription and translation [6] and to characterize subpopulations of CD4 T cells that transcribe HIV RNA [7]. ■

References

1. Deeks SG (2012) *Nature* 487:439–440.
2. Laird GM, Eisele EE, Rabi SA et al. (2013) *PLoS Pathog* 9:e1003398.
3. Trypsteen W, Kiselinova M, Vandekerckhove L et al. (2016) *J Virus Erad* 2:162–169.
4. Procopio FA, Fromentin R, Kulpa DA et al. (2015) *EBioMedicine* 2:874–883.
5. Baxter AE, Niessl J, Fromentin R et al. (2016) *Cell Host Microbe* 20:368–380.
6. Martrus G, Niehrs A, Cornelis R et al. (2016) *J Virol* 90:9018–9028.
7. Grau-Expósito J, Serra-Peinado C, Miguel L et al. (2017) *mBio* 8:e00876-17.

More about the PrimeFlow RNA assay

With the Invitrogen™ PrimeFlow™ RNA Assay Kit, researchers can reveal the dynamics of RNA transcription together with protein expression patterns at the single-cell level by multicolor flow cytometry. The PrimeFlow RNA assay employs fluorescence *in situ* hybridization (FISH) with branched DNA (bDNA) signal amplification for the simultaneous detection of up to 4 RNA targets, and it can be used in combination with immunolabeling of both cell-surface and intracellular proteins using fluorophore-conjugated antibodies.

In the PrimeFlow RNA assay workflow, cells are first labeled with cell-surface antibodies, fixed and permeabilized, and then labeled with intracellular antibodies. Next, these cells are hybridized with oligonucleotide probes specific for the RNA targets. Hybridized targets are detected after bDNA amplification, which is achieved through sequential hybridization steps with preamplifiers, amplifiers, and fluorophore-conjugated label probes. A fully assembled amplification "tree" has 400 label probe–binding sites, and can produce >8,000-fold signal amplification.

With target-specific probe sets, the PrimeFlow RNA assay can be used to detect miRNA, lncRNA, and mRNA, as well as vRNA and telomere DNA. The PrimeFlow RNA Assay Kit provides reagents for detecting up to 4 RNA transcripts in mammalian cells optionally labeled with antibodies that recognize cell-surface or intracellular proteins. For more information, including catalog probe sets and ordering guidelines, visit **thermofisher.com/primeflowbp77**.

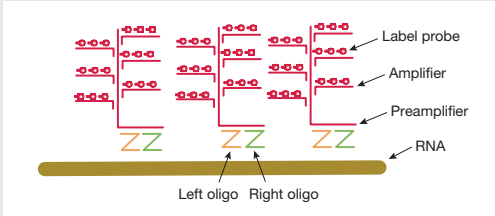

Branched DNA (bDNA) amplification scheme used in the PrimeFlow RNA assay.

Product	Quantity	Cat. No.
PrimeFlow™ RNA Assay Kit	40 tests	88-18005-204
	100 tests	88-18005-210

A comprehensive resource for state-of-the-art flow cytometry methods

Guidelines for the use of flow cytometry and cell sorting in immunological studies.

Cossarizza A, Chang HD, Radbruch A et al. (2017) *Eur J Immunol* 47:1584–1797.

With the advent of monoclonal antibodies conjugated to fluorophores, flow cytometry has become an essential tool for immunological studies. While the flow cytometer is relatively easy to operate, it can be challenging to master the technical aspects—instrument setup, sample preparation, data acquisition, and analysis—to get the most out of flow cytometry experiments. Under the leadership of Andreas Radbruch and Andrea Cossarizza, numerous authorities in the field were invited to share knowledge in their particular area of expertise. As a result of this community effort, the article in the *European Journal of Immunology* aggregates currently accepted methods along with a comprehensive collection of information, protocols, tips, and advice, with the goal of establishing guidelines for the use of flow cytometry and cell sorting in immunological studies.

This article is organized into eight chapters representing key areas of interest, with multiple sections within each chapter. It begins with an overview of flow cytometry equipment, followed by a description of the principles of spectral, imaging, and mass cytometry. Cell sorting, instrument setup, and quality control are discussed, including details on correctly compensating for fluorescence spillover. Fundamentals of experimental design, reagent selection, sample preparation, data acquisition, and cell sorting are each presented, with recommendations for data analysis and handling. The chapter on cytometric parameters includes an extended discussion of 17 different techniques and areas of interest. Perhaps the most interesting to the immunologist is the chapter depicting cytometric phenotypes of 10 cell and tissue types. Finally, a comprehensive list of nearly 1,000 references is included. Here we highlight a few key concepts.

Compensation

Fluorescence spillover, which occurs when a fluorophore's emission is detected in multiple channels, remains a source of frustration for scientists. Correctly compensating for spillover is crucial for accurate population identification, but when performed incorrectly it can lead to poor and even invalid data. A spillover value (SOV) can be calculated using single-color control samples. Compensation is the mathematical process by which the SOVs are used to create a matrix that can be employed to subtract or correct background due to fluorescence spillover.

Four principles for performing compensation are presented: 1) the fluorescence spectrum of a single-color compensation control should be identical to that used in the experiment; 2) autofluorescence of positive and negative populations should be equal; 3) fluorescence of the positive population should be as bright as possible; and 4) at least 5,000 events should be collected in order to calculate an accurate SOV. The use of antibody capture beads, such as Invitrogen™ UltraComp eBeads™ Compensation Beads and Invitrogen™ AbC™ Total Compensation Beads, for single-color compensation controls provides an accurate method for determining fluorescence spillover; moreover, these beads are simple to use and require no biological material, so sample can be conserved.

Sample preparation

Before starting any flow cytometry experiment, reagent and sample preparation should be considered. It is good practice to optimize and validate all reagents used. Just as important is how the cell sample is prepared. A single-cell suspension is required, and therefore techniques for disaggregation (typically mechanical and enzymatic procedures) into single cells are needed when using cells from tissue or adherent cell culture.

When compared with measuring cell-surface targets, the analysis of intracellular targets presents additional challenges and requires fixation and permeabilization procedures. Cell fixation is generally performed using either crosslinking fixatives such as formaldehyde or dehydrating alcohols such as methanol and ethanol. Formaldehyde has the advantage of generally preserving the overall conformation of native proteins, as well as fixing posttranslational modifications and inhibiting the degradation of these targets. Formaldehyde-based reagents such as those found in the Invitrogen™ eBioscience™ Intracellular Fixation and Permeabilization Buffer Set and Invitrogen™ FIX & PERM™ Cell Permeabilization Kit are readily available. →

Mastering the technical aspects of flow cytometry*

Some key takeaways on controls and experiment design.

OBJECTIVE of a flow cytometry experiment: To obtain well-resolved cell populations.

WHAT determines resolution? Resolution is a function of signal separation and spread.

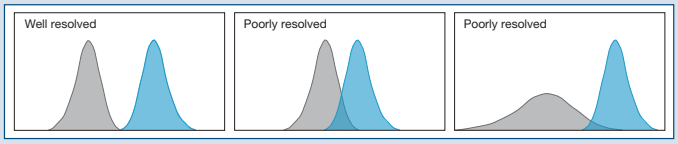

HOW can resolution be enhanced? Fluorophore, sample, and instrument factors affect resolution.

Separating positive and negative signal: Factors that determine separation

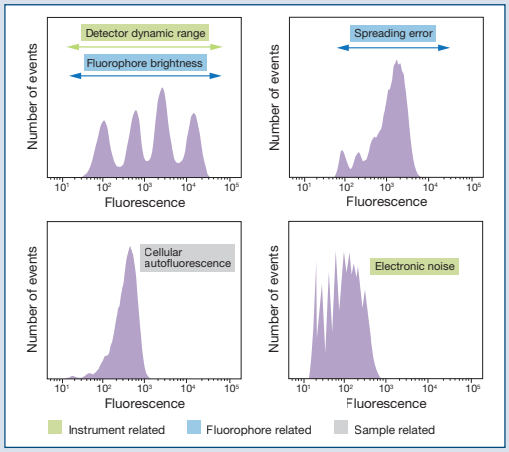

Separating positive and negative signal is critical to accurate detection and interpretation of results. There are multiple sources of fluorescent signal that need to be accounted for, including those from the fluorophore, sample, and instrument.

Determining dye compatibility in multicolor experiments: A spillover-spreading matrix (SSM)

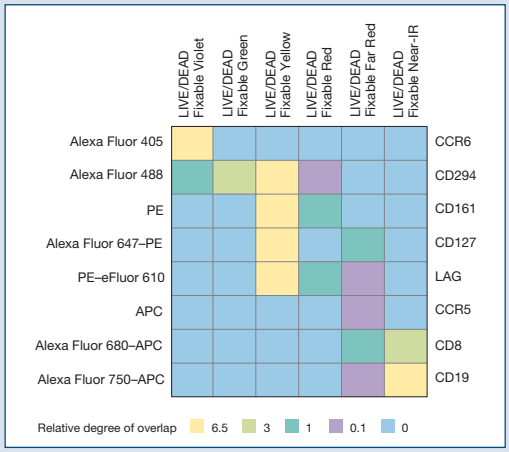

In this hypothetical SSM, emission overlap of several LIVE/DEAD stains is matched to a range of antibody conjugates. The higher the degree of overlap between the stain and antibody conjugate, the greater the spillover.

WHY are these factors important? ↑ Separation + ↓ Spillover = ↑ Resolution

Top 5 compensation mistakes

5. Multiple color controls are analyzed in the same tube instead of individually.
4. An insufficient number of events are collected to obtain an accurate spillover value (SOV); >5,000 events are required.
3. Autofluorescence of the positive and negative controls is not the same.
2. The fluorescence of the positive control is not at least as bright as the biological sample.

And the number 1 compensation mistake is...

1. Use of positive color controls that are spectrally similar—but not identical—to the dyes used in the actual experiment.

*Cossarizza A, Chang HD, Radbruch A et al. (2017) *Eur J Immunol* 47:1584–1797.

Panel design

Advances in hardware and reagent development allow for the detection of up to 30 fluorescence parameters simultaneously, revealing complex biological mechanisms and cell populations. However, they also require the use of a carefully chosen, highly multiplexed antibody panel. Because these panels typically utilize fluorophores that overlap, the principles of single-color compensation controls apply, with the phenomenon known as spreading error (SE) accounted for. SE is an intrinsic characteristic that arises from the counting error associated with low photon numbers. SE is not caused by compensation but it is revealed in compensated data, as the effects of counting error are observed at the low end of a log-scale fluorescence plot. If the SE is very high in a particular detector, a dim marker may not be resolved sufficiently from background signal. Creating a spillover spread matrix (SSM) is useful for characterizing dye and instrument performance and choosing optimal antibody–fluorophore combinations.

Viability assessment

It is essential that the viability of the cell population under examination be known, regardless of the sample preparation method used, and several approaches are discussed. For example, viability assays based on the use of impermeant DNA-binding dyes assess the integrity of the plasma membrane. A healthy intact cell membrane keeps the dye out of the cell, whereas a compromised cell membrane allows the dye to enter the cell, where it binds to the DNA and becomes brightly fluorescent, thus identifying the cell as dead. Impermeant DNA-binding dyes such as propidium iodide (PI), 7-AAD, TO-PRO-3, and the Invitrogen™ SYTOX™ dyes are generally added as the last step in a workflow, and not washed out before data acquisition.

It is important to note that DNA-binding dyes cannot be used on fixed or permeabilized cells. In contrast, protein-binding dyes such as the Invitrogen™ LIVE/DEAD™ and eFluor™ Fixable Dead Cell Stains can be used to assess viability in workflows that require fixation or permeabilization. In cells with compromised membranes, these fixable dyes covalently react with proteins both in the cell interior and on the cell surface, whereas in live cells they only react with cell-surface proteins. The difference in fluorescence intensity is typically on the order of 50-fold, allowing easy discrimination between dead and live cells, and the staining pattern is preserved after fixation. When using protein-binding dyes, it is critical that labeling protocols be performed in the absence of proteins in the staining buffer.

Minimal sample perturbation in ROS evaluation

Reactive oxygen species (ROS) are associated with oxidative stress and include hydrogen peroxide (H_2O_2), superoxide anion ($\cdot O^{2-}$), and hydroxyl radical ($\cdot OH$), which all have relatively short half-lives. Ideally, functional studies for measuring ROS should be performed in whole blood, with minimal sample manipulation, in order to mimic physiological conditions as closely as possible. A no-lyse, no-wash sample preparation method is described that involves simply staining the whole blood sample, diluting it, and then acquiring the sample on the cytometer. Often a fluorescence threshold is set by gating with a CD45 antibody or a vital DNA-binding dye so that only cells of interest are examined. A second approach is discussed that combines the analysis of the blue (488 nm) and violet (405 nm) side scatter laser light; this differential side scatter method allows for detection of red blood cell (RBC), white blood cell (WBC), and platelet populations in the sample because the hemoglobin in RBCs is absorbed by the violet light.

mRNA detection

The immune system comprises heterogeneous cell populations and, upon stimulation, cell-specific responses that trigger production of specialized proteins can be detected at the mRNA level. To fully understand the contribution of cellular heterogeneity to biological function, a single-cell approach is required. Flow cytometry is the gold standard for the study of heterogeneous cell populations. With the novel Invitrogen™ PrimeFlow™ RNA Assay, researchers can detect the dynamics of RNA and protein expression simultaneously using flow cytometry; see “Flow cytometry assay for simultaneous detection of HIV RNA and Gag protein” on page 16. The PrimeFlow RNA assay employs fluorescence *in situ* hybridization (FISH) and branched DNA (bDNA) signal amplification for the detection of up to 4 RNA targets per cell using a standard flow cytometer, and this RNA detection can be combined with immunophenotyping using intracellular and cell-surface antibodies.

Access these guidelines

This publication contains useful information for anyone using flow cytometry as a tool in their research, and it is of particular interest to immunologists. Download this special issue (volume 47, issue 10) of the *European Journal of Immunology,* an open-access publication from the Wiley Online Library, at onlinelibrary.wiley.com/doi/10.1002/eji.201646632/full. ■

Robotic automation for flow cytometry

Attune NxT Flow Cytometer now available with robotic microplate taxiing.

Whether in academic, commercial, or government laboratories, researchers analyzing very large numbers of samples routinely endure time-intensive assays, a requirement to physically monitor the instruments, and susceptibility to human error. Such workflows may be further complicated by instrument instability or clogging and by software malfunctioning. Invitrogen™ flow cytometry products are engineered to operate together seamlessly for automated high-throughput analysis with extended unmanned run time settings, scalable configuration flexibility, and maximized capacity for processing staggering quantities of data.

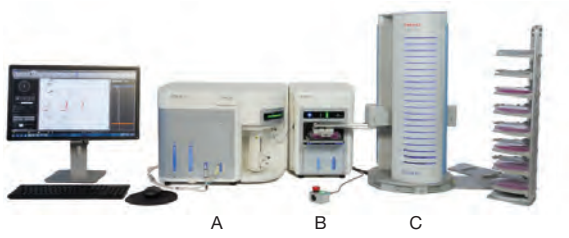

Figure 2. The Attune NxT Flow Cytometer configured for robotic automation with the Orbitor RS Microplate Mover. The components include the **(A)** Attune NxT Flow Cytometer, **(B)** Attune NxT Autosampler, and **(C)** Orbitor RS Microplate Mover.

Multicomponent automated flow cytometry workcell

The robotic automation instrument suite for flow cytometry comprises five benchtop components: flow cytometer, plate sampler, expanded fluidics, robotic arm, and temperature control (Figure 1). The Invitrogen™ Attune™ NxT Flow Cytometer uses acoustics-assisted hydrodynamic focusing technology and is designed to provide faster run times (up to 10 times faster than traditional flow cytometers) and resistance to clogging, even with difficult samples (see the Behind the Bench blog on page 22). Attune NxT accessories expand the functionality of the flow cytometer for high-throughput applications. The Invitrogen™ Attune™ NxT Autosampler, which mixes samples by aspiration rather than shaking, ensures sample homogeneity and is compatible with many plate formats. The Invitrogen™ Attune™ NxT External Fluid Supply facilitates the use of larger buffer and waste containers and monitors the internal fluid tanks of the Attune NxT cytometer over a 24-hour continuous run time.

The Orbitor RS Microplate Mover

The Thermo Scientific™ Orbitor™ RS Microplate Mover is a high-speed microplate mover that offers reliable performance with flexible plate handling. It can keep pace with the already fast Attune NxT cytometer, delivering a plate from storage to instrument in just 4 seconds.

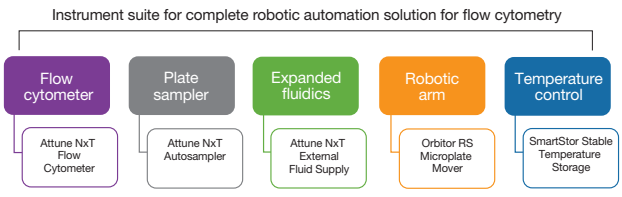

Figure 1. Multicomponent automated flow cytometry workcell.

Moreover, this robot can run unattended, with a continuous run time of up to 19 hours, and has both active and passive safety features, including self-homing, advanced error handling, and collision detection and recovery. Robotic automation for flow cytometry is facilitated by Thermo Scientific™ Momentum™ Laboratory Automation Workflow Software, which connects the Orbitor RS Microplate Mover to the Attune NxT Flow Cytometer and manages operations between the instruments.

The Orbitor RS Microplate Mover can be programmed for multi-step taxiing workflows, operates complex gripping algorithms, and can unlid and relid plates. It includes an integrated barcode reader for plate sensing in the gripper, enabling sample traceability and plate data storage information. The setup of the robotic workcell has flexible options for instrument arrangement and microplate storage, including random-access microplate hotels and sequential-access storage stacks.

Learn more about automation for flow cytometry

Lab automation allows you to maximize operating capacity, mitigate operator error, and collect accurate and reproducible data. Learn more about the multicomponent automated flow cytometry workcell at **thermofisher.com/flowautomationbp77**. There, you can also take 3D instrument tours of the Attune NxT Flow Cytometer and the Orbitor RS Microplate Mover, available in 8 different languages. ■

Product	Quantity	Cat. No.
Attune™ NxT Automation Bundle, stacks	1 bundle	A33007
Attune™ NxT Automation Bundle, hotels	1 bundle	A33008
Attune™ NxT Automation SmartStor Sample Management System	1 system	A35221
Attune™ NxT External Fluid Supply	1 each	A28006

Clog resistance of non–pressure-based flow cytometers

Behind the Bench blog.

Greg Kaduchak, Principal Engineer, Thermo Fisher Scientific.

Clogs in flow cells have been a longstanding issue in flow cytometry. The small dimensions of the flow cell and fluidic path are susceptible to clogs, especially when using larger or "sticky" cells. Furthermore, flow cytometer systems have historically been pressure based, compounding the likelihood of a clog.

Pressure-based flow cytometers

In pressure-based systems, the particles are transported through the system by applying pressure to the fluid. It is a straightforward method to move the fluid through the small channels. To ensure a smooth delivery of fluid and particles through the flow cell without fluctuation, the systems employ pressure regulators. For those that have used these systems, it is a proven design to deliver particles in a flow cytometer and has been successful over the years. In the event of a clog, however, there is not much these systems can do.

Figures 1A and 1B show what happens when a clog is encountered in a pressure-based fluidic system. When the system is in normal operation (Figure 1A), the fluid is pushed through the system at a specified pressure (in this example, 7 psi). But, as seen in Figure 1B, when a clog is encountered the regulator keeps the system at 7 psi. No additional pressure is exerted to move the clog through the flow cell, and in most cases the flow stops.

Fluid displacement–based flow cytometers

In contrast, the pressure is not held constant in systems that employ positive displacement to drive the fluidic system (e.g., syringe pumps). These systems operate using the principle of constant volumetric flow, in which fluid flows with a specified volume delivery rate regardless of the pressure. An example of such a non–pressure-based system facing a potential clog is illustrated in Figures 1C and 1D. When no clog is present (Figure 1C), the system operates at the same pressure as the pressure-based system (here, 7 psi). But once a clog is encountered, pressure will build in the system to maintain the volumetric delivery rate, and this pressure will continue to increase (up to 60 psi) until the clog is displaced (Figure 1D).

The fluidic system in the Attune NxT Flow Cytometer is based on positive displacement fluid delivery. For the purpose of robust clog removal, the system is outfitted with a sensor that monitors the system pressure. When a potential clog is encountered, the pressure is allowed to build to 60 psi before the system safely shuts down. In addition, the Attune NxT Flow Cytometer keeps the flow cell clean by automatically running a rinse cycle between samples, clearing any remaining sample in the flow cell with excess sheath fluid to prevent cellular buildup.

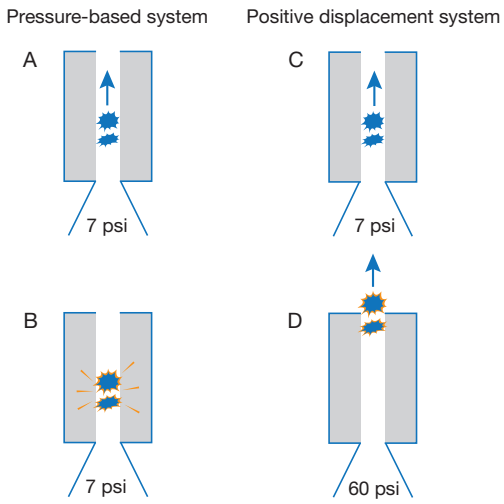

Figure 1. Comparison of pressure-based and positive displacement–based fluidic systems in a flow cytometer. In a pressure-based system, a constant pressure (7 psi) is maintained to move the sample through the system **(A)**, even in the presence of a clog **(B)**. In a positive displacement–based system, a constant pressure (7 psi) moves the sample through the system in the absence of a clog **(C)**, but in the event of a clog, the pressure increases (up to 60 psi) to displace the clog **(D)**.

These features have made the Attune NxT Flow Cytometer extremely clog resistant. Since Thermo Fisher Scientific introduced the Attune NxT Flow Cytometer more than two years ago, users of properly maintained instruments have reported only a very few clogs. Positive displacement systems such as the Attune NxT Flow Cytometer are extremely useful when working with cells that are large and sticky, such as those derived from tissue-based samples. ■

Product	Quantity	Cat. No.
Attune™ NxT Flow Cytometer, blue/red/violet6/yellow	1 each	A29004
Attune™ NxT Flow Cytometer, blue/red/violet6	1 each	A29003
Attune™ NxT Flow Cytometer, blue/violet6	1 each	A29002
Attune™ NxT Violet Laser Upgrade Kit	1 kit	100022777

Tools and protocols for high-content imaging and analysis

Integrating hardware, software, and fluorescent labels for optimized HCA assay development.

- Chambers KM, Mandavilli BS, Dolman NJ, Janes MS (2018) General staining and segmentation procedures for high-content imaging and analysis. *Methods Mol Biol* 1683:21–31.
- Mandavilli BS, Aggeler RJ, Chambers KM (2018) Tools to measure cell health and cytotoxicity using high-content imaging and analysis. *Methods Mol Biol* 1683:33–46.
- Mandavilli BS, Yan M, Clarke S (2018) Cell-based high-content analysis of cell proliferation and apoptosis. *Methods Mol Biol* 1683:47–57.
- Dolman NJ, Samson BA, Chambers KM, Janes MS, Mandavilli BS (2018) Tools to measure autophagy using high-content imaging and analysis. *Methods Mol Biol* 1683:59–71.

High-content imaging and analysis transforms fluorescence microscopy into a high-throughput, quantitative tool for investigating spatial and temporal aspects of cell biology [1]. Automation—not only of the image acquisition but also of the analysis—allows millions of cells to be analyzed and reveals the heterogeneity of responses that exist within cell populations. These cellular responses can then be assessed across a range of manipulations, whether they are genome-wide screens or small-molecule library analyses [2].

To achieve a seamless high-content workflow, automation is required at every step, from image capture to the hardware for scanning microtiter plates and integrating with robotic plate-handling systems. Furthermore, analysis of the acquired images must also be automated; with Thermo Scientific™ HCS Studio™ software, this analysis can occur immediately after capture, producing visible data outputs even as the microplate is scanned.

For those entering the field of high-content imaging, the hardware, software, and reagent considerations can be overwhelming. In a series of recently published reviews in *Methods in Molecular Biology*, Mandavilli and colleagues introduce the essential elements of the high-content imaging and analysis process [3-6]. These reviews provide direction for hardware considerations and software settings, as well as optimized protocols for labeling cells with fluorescent probes. A range of fluorescent probes are discussed, from dyes for labeling cell structures that underpin segmentation to reagents that form the basis of the most commonly used functional assays.

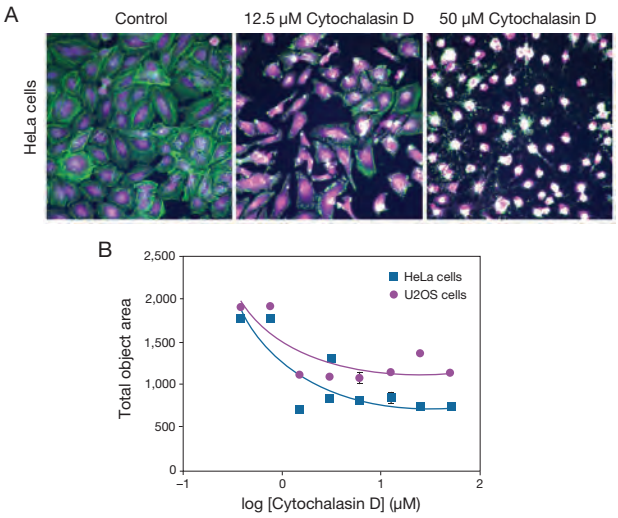

Figure 1. Cytochalasin D disrupts actin filaments and reduces the total area of actin in cells. (A) HeLa or U2OS (images not shown) cells were plated on a 96-well plate at a density of 5,000 cells/well. The cells were treated with different doses of cytochalasin D, from 0.375 µM to 50 µM, for 4 hr. The cells were then fixed, permeabilized, and stained with anti-tubulin antibody (using an Invitrogen™ Alexa Fluor™ 594 secondary antibody) and Invitrogen™ Alexa Fluor™ 488 phalloidin (Cat. No. A12379). After washing, the cells were stained with Invitrogen™ HCS CellMask™ Near-IR stain and Hoechst™ 33342 (Cat. No. H3570), imaged, and analyzed on a Thermo Scientific™ CellInsight™ CX7 LZR High-Content Analysis Platform using a 20x objective. The mean fiber area (actin) was plotted against the cytochalasin D dose.

Segmentation: The cornerstone of high content

High-content imaging and analysis provides automated quantitation of images captured on a fluorescence microscope. Even before the first image is acquired, the high-content analysis (HCA) system must recognize a cell in the field, and this recognition starts with segmentation. Segmentation—the identification of specific elements of the cell—can be achieved through imaging cells stained with fluorescent dyes that selectively label either the nucleus (e.g., Invitrogen™ HCS NuclearMask™ stains) or the entire cell (Invitrogen™ HCS CellMask™ stains). Once the nucleus or cell is recognized as an object to analyze, the software can quantify additional fluorescent reporters for various cellular processes. →

Segmentation based on nuclear labeling enables the HCA software to identify what is or is not a cell. Moreover, the central location of the nucleus within a cell allows cytoplasmic segmentation to be routinely performed without additional labels in the majority of cell types. Chambers et al. [3] provide protocols for labeling cells with the HCS NuclearMask stains, along with optimization approaches based on the types of algorithms selected within HCS Studio software (Table 1). While essential for segmentation, these probes can also offer insight into biological processes. For example, DNA-binding dyes can report DNA content, providing a basis for cell cycle analysis. In addition, the HCS CellMask stains can report changes in cell shape as a function of compound treatment (Figure 1).

HCA assays for cell health and cytotoxicity

One of the most common applications of high-content imaging and analysis is to provide a multiparametric readout of cell health and cytotoxicity. Overall viability assessed using Invitrogen™ LIVE/DEAD™ reagents can be combined with readouts requiring a spatial element, such as probes for mitochondrial membrane potential. Mandavilli et al. describe protocols and trouble-shooting steps for implementing multiparametric probe sets for viability and mitochondrial health, as well as fluorescent probes for determining reactive oxygen species and phospholipidosis/steatosis within cells [4]. For example, the Invitrogen™ HCS Mitochondrial Health Kit provides the reagents required for simultaneous measurement of cell number (blue-fluorescent dye), mitochondrial membrane potential (orange-fluorescent dye), and cell viability (green-fluorescent dye). This approach provides important data when screening for compound toxicity, and even prelethal toxicity. Loss of mitochondrial membrane potential is a common precursor of cell death and is therefore a useful indicator of drug cytotoxicity.

Naturally, some studies require additional assessment of cytotoxicity, and for this reason Mandavilli et al. also provide a detailed discussion regarding the use of Invitrogen™ CellROX™ reagents and Invitrogen™ HCS LipidTox™ stains for measuring reactive oxygen species generation and phospholipidosis/steatosis, respectively, in high-content imaging and analysis applications [4].

Table 1. Nuclear, whole cell, and plasma membrane stains for segmentation.

Segmentation tool	Ex/Em (nm)	Target	Cat. No.
HCS NuclearMask Blue stain	350/461	Nucleus	H10325
HCS NuclearMask Red stain	622/645	Nucleus	H10326
HCS NuclearMask Deep Red stain	638/686	Nucleus	H10294
Hoechst 33342 dye	350/461	Nucleus	H3570
HCS CellMask Blue stain	346/442	Whole cell	H32720
HCS CellMask Green stain	493/516	Whole cell	H32714
HCS CellMask Orange stain	556/572	Whole cell	H32713
HCS CellMask Red stain	588/612	Whole cell	H32712
HCS CellMask Deep Red stain	650/655	Whole cell	H32721
CellTracker Blue CMAC stain	353/466	Whole cell	C2110
CellTracker Blue CMF_2HC stain	371/464	Whole cell	C12881
CellTracker Blue CMHC stain	372/470	Whole cell	C2111
CellTracker Violet BMQC stain	415/516	Whole cell	C10094
CellTracker Green CMFDA stain	492/517	Whole cell	C7025
CellTracker Green BODIPY stain	522/529	Whole cell	C2102
CellTracker Orange CMTMR stain	541/565	Whole cell	C2927
CellTracker Orange CMRA stain	548/576	Whole cell	C34551
CellTracker Red CMTPX stain	577/602	Whole cell	C34552
CellTracker Deep Red stain	630/660	Whole cell	C34565
CellMask Green plasma membrane stain	522/535	Plasma membrane	C37608
CellMask Orange plasma membrane stain	554/567	Plasma membrane	C10045
CellMask Deep Red plasma membrane stain	649/666	Plasma membrane	C10046

HCA assays for cell proliferation, apoptosis, and autophagy

In concert with a suite of advanced fluorescent probes, high-content imaging and analysis can be used to explore mechanistic aspects of cell health, including cell proliferation, apoptosis [5], and autophagy [6]. Proliferation and apoptosis are two key readouts for assessing cell health and are included in established probe combinations for measuring cytotoxicity during compound development and screening [7].

Mandavilli et al. describe the use of a fluorogenic apoptosis probe, Invitrogen™ CellEvent™ Caspase-3/7 Green Reagent, to monitor the early stages of apoptosis [5]. The CellEvent reagent comprises the DEVD peptide—which contains the recognition site for caspase-3 and -7—conjugated to a nucleic acid–binding dye. Because the DEVD peptide inhibits the ability of the dye to bind DNA, CellEvent Caspase-3/7 Green Reagent is intrinsically nonfluorescent. In the presence of activated caspase-3/7, the dye is cleaved from the DEVD peptide and free to bind DNA, producing a bright green-fluorescent signal

(fluorescence emission maximum ~520 nm) indicative of apoptosis (Figure 2A). An important advantage of a fluorogenic probe is that cells do not need to be washed (to remove unbound or unincorporated probe) following incubation. This protocol simplification not only allows preservation of the entire apoptotic population, including fragile cells, which can be lost during wash steps, but also facilitates time-lapse imaging studies, as cells can be imaged in the presence of the probe.

In addition, HCA protocols are described for measuring cell proliferation by labeling cells with the thymidine analog 5-ethynl-2′-deoxyuridine (EdU) and subsequent detection by click chemistry of EdU incorporated into newly synthesized DNA [5], as well as for monitoring the induction of autophagy by immunolabeling cells with an antibody to the autophagosomal marker LC3B [6]. Autophagy is a key pro-survival mechanism implicated in a variety of disease states, including lysosomal storage disorders, neurodegenerative diseases, cancers, and Parkinson's disease [8]. Dolman et al. describe protocols for immunolabeling cells and quantifying LC3B-positive puncta that appear after either blockade of autophagic flux with compounds such as chloroquine or bafilomycin A1, or induction of autophagy through nutrient deprivation or mTOR inhibition (Figure 2B) [6]. Approaches for validating the specificity of autophagosomal labeling using genetic knockout of critical autophagy genes (by CRISPR-Cas9 genome editing) are discussed.

More content about high content

High-content imaging and analysis instruments from Thermo Fisher Scientific—which include the Thermo Scientific™ CellInsight™ CX5 and CellInsight™ CX7 platforms—build on a 20-year legacy of HCA instrument and software development. To find out more about our high-content instrument platforms, software, applications, and analysis reagents, or to request an in-lab demonstration of one of our HCA instruments, visit thermofisher.com/hcabp77. ■

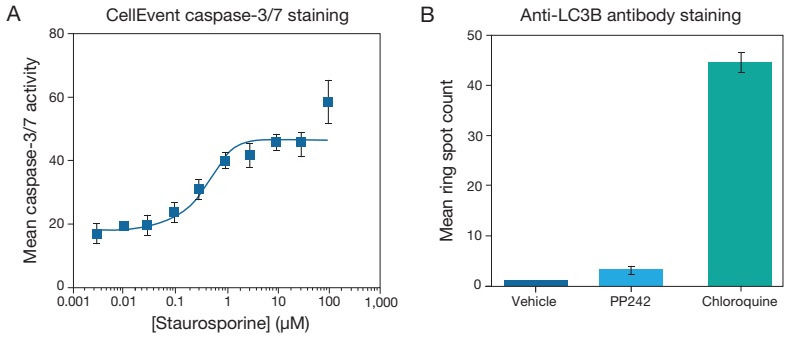

Figure 2. High-content analysis of apoptosis and autophagy. (A) U2OS cells were treated with a range of staurosporine concentrations for 4 hr and then labeled with Hoechst™ 33342 (Cat. No. H3570) and Invitrogen™ CellEvent™ Caspase-3/7 Green Detection Reagent (Cat. No. C10423). The fluorogenic CellEvent reagent reports a dose-dependent increase in induction of apoptosis. **(B)** U2OS cells were treated with either 20 µM chloroquine (to block autophagic flux) or 1 µM PP242 (to stimulate autophagy through mTOR inhibition) and subsequently processed for immunocytochemistry using an antibody against the autophagosomal marker LC3B. Both induction of autophagy and blockade of flux cause a significant increase in the number of autophagosomes detected (LC3B spots). Analysis was carried out using a Thermo Scientific™ CellInsight™ CX5 High-Content Screening Platform.

References

1. Zanella F, Lorens JB, Link W (2010) *Trends Biotechnol* 28:237–245.
2. Nickischer D, Elkin L, Cloutier N et al. (2018) *Methods Mol Biol* 1683:165–191.
3. Chambers KM, Mandavilli BS, Dolman NJ et al. (2018) *Methods Mol Biol* 1683:21–31.
4. Mandavilli BS, Aggeler RJ, Chambers KM (2018) *Methods Mol Biol* 1683:33–46.
5. Mandavilli BS, Yan M, Clarke S (2018) *Methods Mol Biol* 1683:47–57.
6. Dolman NJ, Samson BA, Chambers KM et al. (2018) *Methods Mol Biol* 1683:59–71.
7. Towne DL, Nicholl EE, Comess KM et al. (2012) *J Biomol Screen* 17:1005–1017.
8. Jiang P, Mizushima N (2014) *Cell Res* 24:69–79.

Product	Quantity	Cat. No.
CellInsight™ CX5 High-Content Screening Platform	1 each	CX51110
CellInsight™ CX7 High-Content Analysis Platform	1 each	CX7A1110
CellInsight™ CX7 LZR High-Content Analysis Platform	1 each	CX7A1110LZR
CellEvent™ Caspase-3/7 Green Detection Reagent	100 µL	C10423
CellROX™ Green Reagent	5 x 50 µL	C10444
CellROX™ Orange Reagent	5 x 50 µL	C10443
CellROX™ Deep Red Reagent	5 x 50 µL	C10422
CellROX™ Reagent Variety Pack	1 kit	C10448
Click-iT™ EdU Alexa Fluor™ 488 HCS Assay	2 x 96-well plates	C10350
Click-iT™ EdU Alexa Fluor™ 555 HCS Assay	2 x 96-well plates	C10352
Click-iT™ EdU Alexa Fluor™ 594 HCS Assay	2 x 96-well plates	C10354
Click-iT™ EdU Alexa Fluor™ 647 HCS Assay	2 x 96-well plates	C10356
HCS LipidTOX™ Phospholipidosis and Steatosis Detection Kit	1,200 assays	H34158
HCS LipidTOX™ Green Phospholipidosis Detection Reagent	10 x 96-well plates	H34350
HCS LipidTOX™ Red Phospholipidosis Detection Reagent	10 x 96-well plates	H34351
HCS LIVE/DEAD™ Green Kit	1 kit	H10290
HCS Mitochondrial Health Kit	1 kit	H10295

Advanced laser technology for high-content imaging and analysis

Introducing the CellInsight CX7 LZR High-Content Analysis Platform.

Since the introduction of Thermo Scientific™ high-content imaging and analysis systems in 1999, over 1,000 peer-reviewed publications attest to Thermo Fisher Scientific's legacy of innovation in high-content screening (HCS) and high-content analysis (HCA). This legacy continues with the introduction of the Thermo Scientific™ CellInsight™ CX7 LZR High-Content Analysis Platform, an updated version of our CellInsight CX7 instrument with advanced laser technology.

High-content analysis comprises a combination of fluorescence microscopy, image processing, automated cell measurements, and informatics tools that has enabled significant progress in both basic research and drug discovery. Providing the resolution of microscopy with the statistical power inherent in a highly quantitative analysis, HCA platforms have been fundamental in applications ranging from toxicology assays to cell phenotyping.

Meet the CellInsight CX7 LZR HCA Platform

The CellInsight CX7 LZR HCA Platform (Figure 1) delivers superior performance for the diverse set of experiments and cell types that are emerging in cell-based assays and provides a broad set of tools for quantitative imaging and analysis. This integrated benchtop system offers widefield, confocal (critical for 3D acquisition), and brightfield imaging with extremely bright illumination to penetrate thick samples. It also provides fast image acquisition with shorter exposure times and laser autofocus capabilities. Live-cell imaging and analysis benefit from the expanded multiplexing options provided by the near-infrared (785 nm) laser, and from advanced features that allow you to control the amount of light reaching the sample, helping to minimize photobleaching and phototoxicity. In addition, the CellInsight CX7 LZR HCA Platform has been designed to provide:

- Microscope objectives from 2x to 60x
- A broad range of compatible plate formats and types
- Seamless data sharing and storage using Thermo Scientific™ Store Image and Database Management Software
- Optional onstage incubation and robotic plate handling

Take advantage of the onboard HCS Studio software

Thermo Scientific™ HCS Studio™ Cell Analysis Software is the engine behind all of our high-content imaging and analysis systems, including the CellInsight CX7 LZR HCA Platform. The HCS Studio software allows access to all instrument configuration and control functions, working in concert with Store Image and Database Management Software to analyze and store the resulting high-content images and data. Data acquisition with the HCS Studio software is intelligent, collecting data cell by cell until statistically relevant results can be reported for the assay parameters.

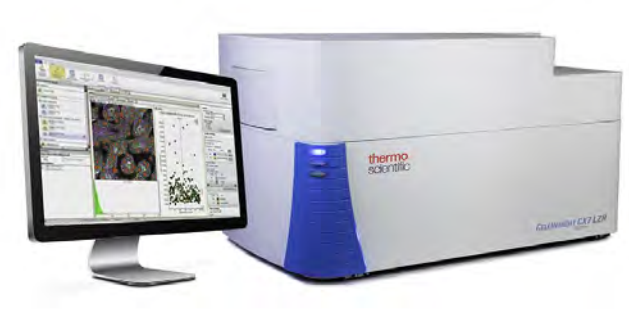

Figure 1. CellInsight CX7 LZR High-Content Analysis Platform.

This intuitive, icon-driven tool helps to manage the experimental design and workflow, starting with plate maps and protocol setup, all the way through image acquisition and data analysis. You can configure your assay quickly using the simple, icon-based interface, and image acquisition is fully automated even when multiple channels and imaging modes are required. Once images are acquired, users can leverage the software's suite of available bioapplications, purpose-built for specific biological areas such as proliferation, translocation, neurite outgrowth, apoptosis (Figure 2), and autophagy. Data are processed in real time with no manual intervention required, allowing you to go from image collection to tabulated results and population statistics in minutes.

HCA Onstage Incubator for live-cell imaging

The Invitrogen™ HCA Onstage Incubator is an optional accessory that allows you to equip your CellInsight instrument with live-cell imaging capabilities, enabling quantitation of biological processes in a controlled environment over an extended period of time. The HCA Onstage Incubator allows precise control of temperature, humidity, and CO_2 levels. It also contains integrated scheduling software for kinetic and motility measurements, as well as robot compatibility for fixed-endpoint assays and the capability to generate multicolor movies.

Add high-content capabilities to your lab

The CellInsight CX7 LZR HCA Platform provides an integrated benchtop instrument that interrogates multiple sample types with a wide range of techniques and takes advantage of next-level image acquisition and analysis software. This high-content imaging and analysis technology builds on a 20-year legacy of instrument and software development and over 40 years of fluorescence imaging and probe development in our cell and protein analysis laboratories. To find out more about our high-content imaging and analysis platforms, software, applications, and analysis reagents, or to request an in-lab demonstration, visit thermofisher.com/hcabp77. ■

Product	Quantity	Cat. No.
CellInsight™ CX7 LZR High-Content Analysis Platform	1 each	CX7A1110LZR
CellInsight™ CX7 LZR High-Content Analysis Platform and Store Standard Edition (SE) software	1 each	CX7B1112LZR
CellInsight™ CX7 LZR High-Content Analysis Platform with Store Standard Edition (SE) software and Orbitor™ RS Plate Mover	1 each	CX7C1115LZR
HCA Onstage Incubator for CellInsight™ CX7 and CX7 LZR instruments	1 each	NX7LIVE001

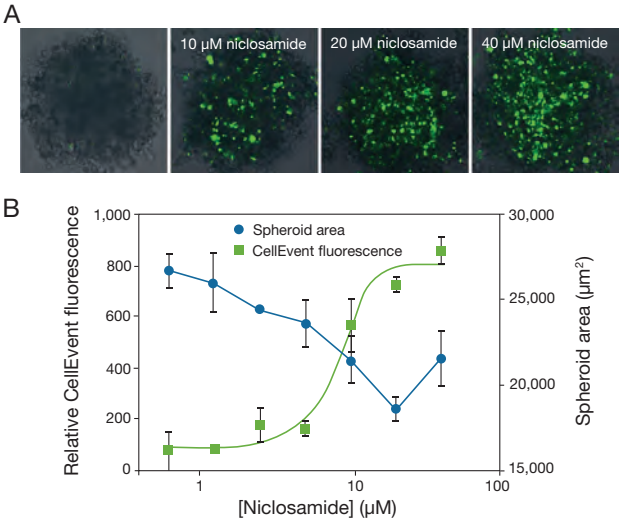

Figure 2. Detection of apoptosis in A549 spheroids treated with niclosamide. A549 cells were plated in 96-well U-bottom plates for spheroid growth and left in the CO_2 incubator for 24 hr. The resulting spheroids were left untreated or treated with niclosamide (0.3 µM to 40 µM) for 24 hr. To detect apoptosis, spheroids were stained with 2 µM CellEvent Caspase-3/7 Green Detection Reagent (Cat. No. C10423) for 1 hr and imaged on a Thermo Scientific™ CellInsight™ CX7 LZR HCA Platform using brightfield and confocal modes with a 10x objective. **(A)** The images are the maximum intensity projections of 16 different Z slices. **(B)** CellEvent fluorescence and spheroid area were plotted against niclosamide concentration.

Versatile western blot transfer system: Performance coupled with flexibility

The Invitrogen™ Power Blotter System is a flexible solution for western blot transfer, from interchangeable blotting cassettes to suit your required throughput, to multiple transfer stack choices. The Power Blotter utilizes an integrated power supply, LCD touchscreen, and preprogrammed, optimized protocols for rapid, efficient semi-dry transfer of proteins from gels to membranes. For transferring up to 2 mini gels or 1 midi gel simultaneously, choose the standard Power Blotter System; for greater transfer capacity, choose the Power Blotter XL System, which can transfer up to 4 mini gels or 2 midi gels at once. Learn more about adding the Power Blotter to your western blotting workflow at thermofisher.com/powerblotter. In addition, see "Innovative western blotting from start to finish" on page 28.

Product	Quantity	Cat. No.
Power Blotter System (Power Blotter Station and Power Blotter Cassette)	1 system	PB0012
Power Blotter Welcome Pack, including Power Blotter System and transfer stacks, membranes, filters, and buffer	1 kit	PB0112
Power Blotter XL System (Power Blotter Station and Power Blotter XL Cassette)	1 system	PB0013
Power Blotter XL Welcome Pack, including Power Blotter XL System and transfer stacks, membranes, filters, and buffer	1 kit	PB0113

Power Blotter System (top) and Power Blotter XL System (bottom).

Innovative western blotting from start to finish

Introducing the four-component iWestern Workflow Bundle.

Streamline your western blotting with the Invitrogen™ iWestern™ Workflow, an inventive take on the decades-long problem of getting the desired results from the often elusive and time-consuming western blot. Every instrument in the iWestern Workflow is meticulously developed to produce exceptional western blot results with minimal hands-on time. At the core of the iWestern Workflow are four innovative western blotting instruments designed with a focus on processing efficiency, reproducibility, and performance (Figure 1).

Figure 1. iWestern Workflow instrument components. From left to right, the Invitrogen™ Mini Gel Tank, the Invitrogen™ iBind™ Western Device, the Invitrogen™ iBlot™ 2 Gel Transfer Device, and the Invitrogen™ iBright™ FL 1000 Imaging System.

Separate proteins

The Invitrogen™ Mini Gel Tank is an intelligently engineered protein electrophoresis tank with a side-by-side design that provides a forward-facing well configuration for easier sample loading and simultaneous visualization of both gels during electrophoresis. Because it has two individual buffer tanks, less running buffer is required when running only a single gel. Compatible with over 180 gels of different formats and gel chemistries, the Mini Gel Tank provides the flexibility to choose the best gel for the experiment at hand.

We provide the Mini Gel Tank in each of our Protein Gel Welcome Packs (Figure 2). Protein Gel Welcome Packs include two boxes of gels (with your choice of gel chemistry) and the necessary buffers to perform electrophoresis. The standard iWestern Workflow Bundle includes the Invitrogen™ Bolt™ Gel Welcome Pack, featuring Bis-Tris gel chemistry for optimal western blotting performance. You can also customize your iWestern Workflow Bundle by choosing an alternative Protein Gel Welcome Pack with gel chemistry that is compatible with your target protein's abundance and size, and the downstream application (Table 1).

Table 1. Precast gels available with four gel chemistry options to fit your protein separation needs.

Gel chemistry	Application
Bis-Tris	Broad-range, low-abundance protein separation; downstream applications requiring high protein integrity (e.g., posttranslational modification analysis, mass spectrometry, or sequencing)
Tris-glycine	Broad-range, high-abundance protein separation
Tris-acetate	High molecular weight protein separation (up to 500 kDa)
Tricine	Low molecular weight protein separation (as low as 2 kDa)

Transfer proteins

The Invitrogen™ iBlot™ 2 Gel Transfer Device is our premium western blot transfer device, delivering high performance and convenience. The iBlot 2 Gel Transfer Device is a unique, innovative dry blotting system that utilizes preassembled transfer stacks with transfer buffer incorporated into gel matrices, so there is no need to prepare messy transfer buffers, and minimal posttransfer cleanup is required. The short distance between electrodes, along with high field strength and current, reduces transfer time to only 7 minutes—just insert your gel and go. The standard iWestern Workflow Bundle includes the iBlot 2 Starter Kit (Figure 3), with transfer stacks to get you started.

Detect proteins

The Invitrogen™ iBind™ Western Devices are simple, nonpowered instruments that automate many of the tedious, routine western blot processing steps and improve blot-to-blot consistency. The original iBind Western Device accommodates the processing of one mini blot at a time, whereas the iBind Flex Western Device accommodates the processing of up to one midi blot, two mini blots, or six vertically cut strip blots. Both systems are compatible with chromogenic, chemiluminescence, and fluorescence detection protocols.

Simply load primary antibody, secondary antibody, and wash solutions, then walk away. Sequential lateral flow technology takes over, eliminating the need for trays, timers, or shakers. The entire immunoblotting process is complete in less than 3 hours and uses up to 80% less primary antibody than traditional methods. The standard iWestern Workflow Bundle comes with the iBind Starter Kit (Figure 4), which includes the consumables needed to get started, but it can be customized to include the iBind Flex Starter Kit if increased throughput is needed.

Image and analyze proteins

The Invitrogen™ iBright™ Imaging Systems (Figure 5) are high-performance, all-in-one instruments for capturing images and analyzing data from western blots and gels. Complete with a powerful 9.1 megapixel camera (Figure 6), proprietary Smart Exposure™ acquisition technology, Thermo Fisher Cloud connectivity, an easy-to-use interface, and a suite of automated features, iBright Imaging Systems make western blot imaging fast and easy for researchers at all experience levels.

Two iBright instruments are available—the iBright CL1000 system, for imaging and documenting chemiluminescent western blots and stained protein and nucleic acid gels, and the iBright FL1000 system (Figure 5), which features the same imaging modes as the iBright CL1000 system but also offers 5-channel fluorescent blot imaging capability in both visible and near-IR excitation and emission channels. The standard iWestern Workflow Bundle includes the iBright FL1000 Imaging System.

Modernize your western blot protocol with the iWestern Workflow

Learn more about the iWestern Workflow Bundle, explore the many options for customization, and request a quote at thermofisher.com/iwesternbp77. ■

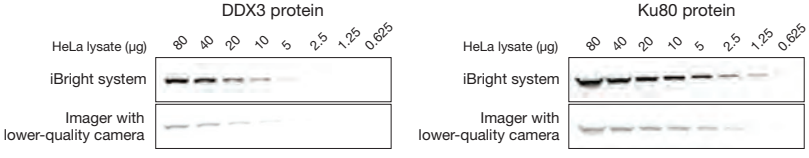

Figure 6. iBright Imaging Systems feature a powerful 9.1 megapixel camera for sensitive signal detection. Two-fold serial dilutions of HeLa cell lysate (starting at 80 µg/lane) were loaded and run on Invitrogen™ Novex™ Tris-glycine gels, transferred, and probed with antibodies against DDX3 or Ku80 protein. Blots were then probed with corresponding HRP-conjugated secondary antibodies, developed with Thermo Scientific™ SuperSignal™ West Pico PLUS Chemiluminescent Substrate (Cat. No. 34577), and visualized (using 10 sec exposures) on either the Invitrogen™ iBright™ FL1000 Imaging System or another imaging device with a lower-quality, 4.1 megapixel camera.

Figure 2. Protein Gel Welcome Pack with Mini Gel Tank.

Figure 3. Invitrogen™ iBlot™ 2 Starter Kit.

Figure 4. Invitrogen™ iBind™ Starter Kit.

Figure 5. Invitrogen™ iBright™ FL1000 Imaging System.

Assay RNA quality with the updated Qubit benchtop fluorometer

Introducing the Qubit 4 Fluorometer and Qubit RNA IQ Assay.

The Invitrogen™ Qubit™ 4 Fluorometer is the newest generation of the popular benchtop fluorometer designed to quantify DNA, RNA, and protein using the highly sensitive Invitrogen™ Qubit™ assays. This latest version of the Qubit fluorometer has been reengineered to run the Invitrogen™ Qubit™ RNA IQ Assay for assessing RNA integrity and quality. The Qubit 4 Fluorometer and Qubit RNA IQ Assay work together to accurately distinguish viable from degraded RNA in just a few simple steps: mix reagent, add sample, and read.

Qubit 4 Fluorometer

As with its predecessors, the Qubit 4 Fluorometer (Figure 1) provides sensitive and accurate detection and quantitation of DNA, RNA, and protein using 1 to 20 µL of sample. For over a decade, life science researchers have relied on the Qubit fluorometer when handling valuable or complex samples (e.g., blood or formalin-fixed, paraffin-embedded (FFPE) tissue), and when preparing samples for critical downstream applications such as next-generation sequencing (NGS)—particularly in cases when UV absorbance is unable to accurately detect the concentration or to discern between RNA and DNA (Figure 2). With easy-to-use touchscreen menus, state-of-the-art algorithms, and Wi-Fi connectivity, the Qubit 4 Fluorometer quickly and accurately quantifies DNA, RNA, and protein, with a read time of less than 3 seconds per sample, and can store up to 1,000 sample results.

Qubit RNA IQ Assay

The updated Qubit 4 Fluorometer is designed to enable RNA qualification with the Qubit RNA IQ (Integrity & Quality) Assay, which distinguishes between intact and degraded RNA. In contrast with classic gel or capillary electrophoresis methods, the Qubit RNA IQ Assay utilizes two unique fluorescent dyes to assess whether the RNA sample is viable for use or degraded. One dye binds to large intact RNA with or without secondary or tertiary structure; the second dye selectively binds to small, degraded RNA. To perform the RNA IQ assay, simply prepare the RNA IQ working solution, add samples, and then measure the signal using the Qubit 4 Fluorometer. No special handling, tedious sample preparation, or waiting for results are required. With as little as 1 µL of your sample (containing 0.5–1.5 µg RNA), you can determine the quality and integrity of the sample RNA in just a few seconds.

The Qubit 4 Fluorometer reports the results from the RNA IQ assay as an RNA IQ value, which is based on a scale of 1 to 10 and is similar to RNA quality scores used in other methods. A high IQ value indicates that the majority of the sample consists of large or structured RNA; a low IQ value indicates that the sample contains small RNA with limited secondary and tertiary structure (Figure 3). Additionally, both of the fluorescent dyes used in the RNA IQ assay emit signal only when bound to the target molecule, minimizing the impact of contaminants on the readout accuracy.

Better DNA and RNA quantitation

In addition, we have developed improved versions of the classic Qubit DNA and RNA quantitation assays. The updated Invitrogen™ Qubit™ 1X dsDNA HS (high sensitivity) Assay provides the reagents in a ready-to-use formulation that is stable for up to 1 year at 2–8°C. This new Qubit 1X dsDNA assay provides the same dynamic range (10 pg/µL to 100 µg/µL), limit of detection (0.2 ng), and accurate results at very low DNA concentrations as the original Qubit dsDNA HS Assay (Figure 4).

Figure 1. Qubit 4 Fluorometer.

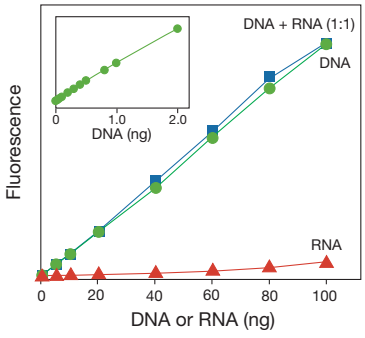

Figure 2. Performance of the Qubit dsDNA HS Assay. The Invitrogen™ Qubit™ dsDNA HS Assay has a linear detection range of 0.2–100 ng and is selective for dsDNA, even in the presence of an equal mass of RNA.

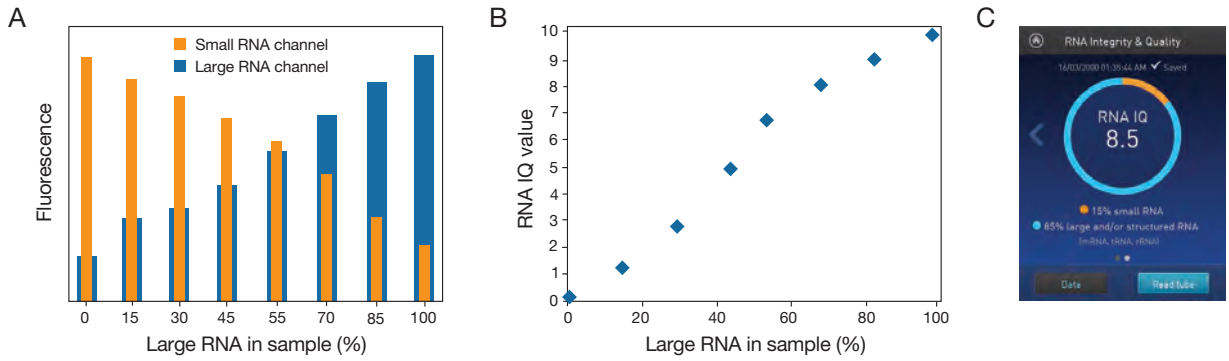

Figure 3. Qubit RNA IQ fluorescence response and IQ value for solutions containing various proportions of large and small RNA. Triplicate samples containing a total of 100 ng/mL RNA, comprising small RNA (Invitrogen™ Silencer™ Select GAPDH Positive Control siRNA, Cat. No. 4390849) and large RNA (*E. coli* rRNA), were assayed with the Invitrogen™ Qubit™ RNA IQ Assay (Cat. No. Q33221, Q33222) on the Invitrogen™ Qubit™ 4 Fluorometer. **(A)** Relative fluorescence and **(B)** RNA IQ values were plotted for all samples. **(C)** A Qubit 4 Fluorometer readout shows the RNA IQ assay results for one sample.

The Invitrogen™ Qubit™ RNA XR (extended range) Assay can detect up to 8 µg of RNA, whereas the Invitrogen™ Qubit™ RNA BR (broad range) Assay is only able to detect a maximum of 1 µg. Both Qubit RNA assays provide the same lower limit of detection (20 ng).

The Qubit 1X dsDNA HS and Qubit RNA XR Assays are preprogrammed on the Qubit 4 Fluorometer. If you already have a Qubit 2 or Qubit 3 Fluorometer, programs for these assays can be downloaded at **thermofisher.com/qubit**. The improved dsDNA and RNA assays are also available as Invitrogen™ Quant-iT™ Assay Kits, which are optimized for use with fluorescence microplate readers (but can also be used on the Qubit fluorometer) and include 8 standards.

Get started with a Qubit Starter Kit

The Qubit Starter Kits provide a convenient and efficient way to get started with Qubit DNA, RNA, or protein quantitation. They include a Qubit 4 Fluorometer, Qubit quantitation kit(s), and Qubit assay tubes. Visit **thermofisher.com/qubitbp77** for more information about the Qubit 4 Fluorometer, the Qubit RNA IQ Assay, and the family of Qubit and Quant-iT quantitation assays. ■

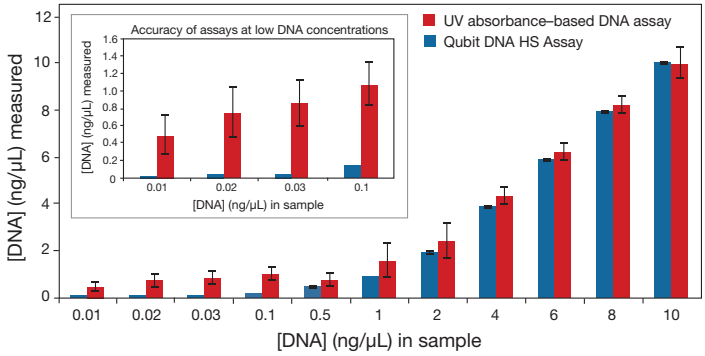

Figure 4. Accuracy and precision of the Qubit Quantitation Platform. Ten replicates of lambda DNA at concentrations from 0.01 to 10 ng/µL were assayed using the Invitrogen™ Qubit™ dsDNA HS Assay on the Invitrogen™ Qubit™ Fluorometer according to the standard kit protocol. The same concentrations of DNA were assayed in 10 replicates using UV absorbance measurements and a microvolume spectrophotometer, and results were compared for both accuracy and precision. Each bar represents the average of 10 replicates. Error bars represent the standard deviations of the 10 replicates. The concentrations indicated are the concentrations of DNA in the starting samples, before dilution in the Invitrogen™ Qubit™ Assay Tubes (Cat. No. Q32856).

Product	Quantity	Cat. No.
Qubit™ 4 Fluorometer and starter kits		
Qubit™ 4 Fluorometer	1 fluorometer	Q33226
Qubit™ 4 Quantitation Starter Kit	1 fluorometer, 6 kits	Q33227
Qubit™ 4 NGS Starter Kit, for next-generation sequencing	1 fluorometer, 1 kit	Q33228
Qubit™ 4 RNA IQ Starter Kit, for RNA integrity & quality	1 fluorometer, 1 kit	Q33229
Qubit™ RNA and DNA assays		
Qubit™ RNA IQ Assay	1 kit, 75 assays 1 kit, 275 assays	Q33221 Q33222
Qubit™ RNA XR Assay Kit	1 kit, 100 assays 1 kit, 500 assays	Q33223 Q33224
Quant-iT™ RNA XR Assay Kit*	1 kit, 1,000 assays	Q33225
Qubit™ 1X dsDNA HS Assay Kit	1 kit, 100 assays 1 kit, 500 assays	Q33230 Q33231
Quant-iT™ 1X dsDNA Assay Kit*	1 kit, 1,000 assays	Q33232

*To use a Quant-iT assay on a Qubit Fluorometer, simply replace standards 1 and 2 with standards 1 and 8 from the Quant-iT assay.

A view of the steady-state distributions of proteins within a cell

Using hyperLOPIT to perform high-resolution mapping of the spatial proteome.

Mulvey CM, Breckels LM, Geladaki A, Britovšek NK, Nightingale DJH, Christoforou A, Elzek M, Deery MJ, Gatto L, Lilley KS (2017) *Nat Protoc* 12:1110–1135.

Eukaryotic cell health is dependent on the spatial and temporal organization of proteins that control cell growth, division, metabolism, and other vital processes. The specific subcellular localization of a protein can not only regulate its activity but also determine its function and downstream effects. Aberrant protein localization has been implicated in a diverse array of human diseases, including neuronal degeneration and cancer [1]. Protein localization has traditionally been studied using fluorescence microscopy in conjunction with GFP-tagged fusion proteins or fluorophore-labeled antibodies. However, these methods have limited throughput and are dependent on the generation of recombinant proteins or the availability of specific antibodies.

To obtain a more complete view of the spatial proteome, Dr. Kathryn Lilley and colleagues developed LOPIT (localization of organelle proteins by isotope tagging), which combines cell fractionation using density-gradient ultracentrifugation with multiplex quantitative mass spectroscopy [2]. In the LOPIT method, cellular proteins are first separated into various subcellular fractions based on their density. Each fraction is then labeled with stable isotope–encoded chemical tags that facilitate the measurement of abundance (and localization) of hundreds of proteins relative to organelle marker proteins.

In their 2017 article, Mulvey et al. describe their updated higher-multiplex LOPIT (hyperLOPIT) protocol that enables high-resolution mapping of thousands of proteins in a single experiment [3]. The hyperLOPIT protocol integrates improved fractionation strategies with technological advances in stable isotope tag labeling and mass spectrometry acquisition methods, increasing both the number of proteins analyzed per run and the granularity of protein localization to suborganelles and large protein complexes. The hyperLOPIT technique overcomes many of the limitations of the original LOPIT method, which only examined integral membrane proteins (not soluble or peripheral membrane proteins) in a few subcellular compartments, and resulted in suboptimal quantitation arising from the mass spectrometry analysis methods available at the time. In addition to optimized fractionation and mass spectrometry methods for higher-plex sample analysis, the hyperLOPIT workflow includes machine learning–based analysis of the spatial proteomics data (Figure 1).

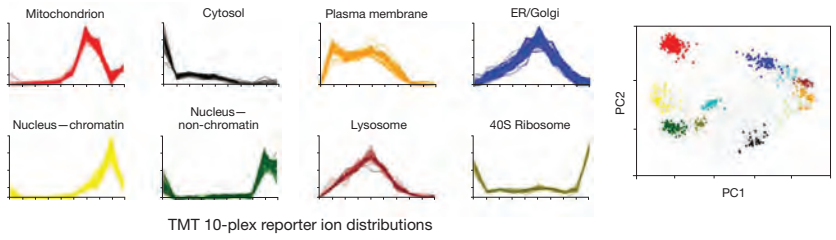

Figure 1. hyperLOPIT data analysis. Subcellular fractionation of E14TG2a murine embryonic stem cells using density-gradient ultracentrifugation coupled with isobaric mass tagging and synchronous precursor selection (SPS) MS^3 mass spectrometry produced spatial proteome maps of cellular proteins. Machine learning and data analyses are performed using pRoloc software (**bioconductor.org/packages/pRoloc**) to assign the protein profiles of unknown location to the profiles of well-known organelle markers. Line graphs (left) showing TMT reporter ion distributions for 8 organelles demonstrate that colocalized proteins exhibit similar profile patterns in the gradient. The multivariate data set can be visualized in 2D using principal component analysis (PCA, right) to provide a view of organelle separation and subcellular resolution; each point represents one protein and is colored according to its subcellular niche. Reproduced with permission from Christoforou A et al. (2016) *Nat Commun* 7:9992 and under the Creative Commons Attribution 4.0 International License (**creativecommons.org/licenses/by/4.0/**).

Mulvey et al. provide a visual step-by-step hyperLOPIT protocol with estimated time to complete each step, as well as a comprehensive list of reagents and equipment. Also included is a troubleshooting guide and links to a downloadable, open-source computational toolkit that includes pRoloc and pRolocGUI for the statistical analysis and interactive visualization, respectively, of spatial proteomics data. Although the hyperLOPIT method was developed using the mouse embryonic stem cell line E14TG2a [4], the authors state that it can be used to produce a spatial map of any cell line or homogeneous tissue, as long as the cells can be lysed without compromising the integrity of organelle membranes. Overall, the use of hyperLOPIT to create high-resolution maps of protein localization is a breakthrough in spatial proteomics that will contribute greatly to our understanding of cell function, organization, and disease states. ■

References

1. Hung MC, Link W (2011) *J Cell Sci* 124: 3381–3392.
2. Sadowski PG, Dunkley TP, Shadforth IP et al. (2006) *Nat Protoc* 1:1778–1789.
3. Mulvey CM, Breckels LM, Geladaki A et al. (2017) *Nat Protoc* 12:1110–1135.
4. Christoforou A, Mulvey CM, Breckels LM et al. (2016) *Nat Commun* 7:9992.

Cover image

Chimeric antigen receptor (CAR) T cell invasion into cancer spheroids. HCC827 spheroids were formed using spheroid microplates for 48 hr. Then, 24 hr after the addition of EGFR scFv-CD28-CD3ε CAR T cells (ProMab Biotechnologies), spheroids were immunostained for cytokeratin-7 (green) and CD3ε (red), and counterstained with Hoechst™ dye (blue). As the effector-to-target ratio is increased from 10:1 to 40:1, invasion of the CAR T cells into the HCC827 tumor spheroid and subsequent tumor cell lysis are visible; shown here is an effector-to-target ratio of 10:1. Images were obtained on the Thermo Scientific™ CellInsight™ CX7 High-Content Analysis Platform in confocal mode with a 10x objective and used with permission from Corning Inc. For more details, see "Immuno-oncology: Advances in basic research and translational medicine" starting on page 8.

Previous issues

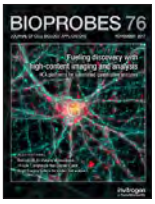

BIOPROBES 76

This issue highlights recent publications citing the use of Thermo Scientific™ high-content analysis (HCA) platforms. Also discussed are fluorescent probes for autophagy, antibody internalization, and low-density lipoproteins, as well as a 14-color T cell immunophenotyping flow cytometry panel, ProQuantum™ immunoassays, and the iBright™ Imaging Systems for western blot analysis.

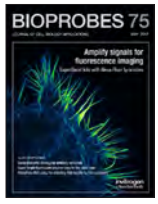

BIOPROBES 75

In this issue, we describe SuperBoost™ Kits with Alexa Fluor™ tyramides for signal amplification, as well as immune checkpoint antibodies, Super Bright antibody conjugates for the violet laser, and the PrimeFlow™ RNA assay for detecting RNA targets by flow cytometry. A center insert includes a fluorophore and reagent selection guide for flow cytometry.

BIOPROBES 74

This issue focuses on CRISPR-Cas9–based research, including the combination of genome editing and functional proteomics, as well as a description of our comprehensive portfolio of reagents for Cas9 delivery through cell function assays. Also highlighted are several stem cell studies and fluorescent reagents for flow cytometry and imaging, such as the FluxOR™ II Green K^+ channel assay.

Back issues of *BioProbes Journal* published after 1995 are available at **thermofisher.com/bioprobes**. Subscribe to *BioProbes Journal* at **thermofisher.com/subscribebp**.

Thermo Fisher Scientific

5781 Van Allen Way
Carlsbad, California 92008
United States
Tel: +1 760 603 7200
Toll-Free Tel: 800 955 6288
Fax: +1 760 603 7229
Email: techsupport@thermofisher.com

2014 APEX® AWARDS FOR PUBLICATION EXCELLENCE

For Research Use Only. Not for use in diagnostic procedures.

COL06302 0518

thermofisher.com/bioprobes

Thermo Fisher Scientific
4401 E Marginal Way S
Seattle, WA 98134

Evolutionary technology. Revolutionary potential.

Designed to help you realize the full potential of flow cytometry, the Invitrogen™ Attune™ NxT Flow Cytometer is modern technology for today's science—and tomorrow's discoveries. Welcome to a new era in flow cytometry.

Explore all features at **thermofisher.com/attune**

ThermoFisher SCIENTIFIC

invitrogen

Fluorophore and reagent selection guide for flow cytometry

The Invitrogen™ Attune™ NxT Flow Cytometer.

For more information, go to **thermofisher.com/attune**

Excitation laser	Common emission filters (nm)	Attune NxT channel (nm)*	Recommended dyes	Viability dyes (compatible with fixation)	Viability dyes (unfixed cells)	DNA content/ cell cycle dyes (live cells)	DNA content/ cell cycle dyes (fixed cells)	Apoptosis dyes	Cell proliferation dyes	Reactive oxygen species (ROS) dyes	Phagocytosis dyes	Fluorescent proteins	Other dyes
UV (~350 nm)	379/28	NA											BD Horizon BUV395
	440/40 450/50	NA	Alexa Fluor 350 Alexa Fluor 405	LIVE/DEAD Fixable Blue	DAPI SYTOX Blue	Hoechst 33342 Vybrant DyeCycle Violet	FxCycle Violet (DAPI)	Annexin V, Alexa Fluor 350 Annexin V, Pacific Blue	CellTrace Blue Click-iT Plus EdU Alexa Fluor 350			ECFP	BD Horizon BUV496
	740/35	NA											BD Horizon BUV737
Violet (405 nm)	425/20 440/50 450/50 455/50 450/65 460/50	VL1 440/50 VL1 (V6**) 450/40	Super Bright 436 eFluor 450 Pacific Blue Alexa Fluor 405	LIVE/DEAD Fixable Violet	DAPI SYTOX Blue	Vybrant DyeCycle Violet	FxCycle Violet (DAPI)	Annexin V, Pacific Blue Annexin V, eFluor 450 PO-PRO-1	CellTrace Violet Click-iT Plus EdU Pacific Blue			Azurite Cerulean TagBFP ECFP mTurquoise AmCyan	BD Horizon BV421 BD Horizon V450 VioBlue
	510/50 520/35 525/50 530/40 550/40	VL2 512/25 VL2 (V6) 525/50	eFluor 506 Pacific Green	LIVE/DEAD Fixable Aqua				Violet Ratiometric Probe (F2N12S)				T-Sapphire	BD Horizon BV510 BD Horizon V500 VioGreen
	585/40 610/20	VL3 603/48 VL3 (V6) 610/20	Super Bright 600 Pacific Orange Qdot 605	LIVE/DEAD Fixable Yellow				Violet Ratiometric Probe (F2N12S)					BD Horizon BV570 BD Horizon BV605 BD Horizon BV650
	660/20 660/40 710/50	VL4 710/50 VL4 (V6) 660/20	Super Bright 645 Super Bright 702 Qdot 705										BD Horizon BV650 BD Horizon BV711
	710/50	VL5 710/50	Super Bright 702										BD Horizon BV711
	780/60	VL6 780/60	Super Bright 780										BD Horizon BV786
Blue (488 nm)	525/50 525/30 525/40 530/30 530/40	BL1 530/30 BL1 (G†) 525/50	Alexa Fluor 488 FITC	LIVE/DEAD Fixable Green	SYTOX Green	Vybrant DyeCycle Green		Annexin V, Alexa Fluor 488 Annexin V, FITC APO-BrdU TUNEL with Alexa Fluor 488 CellEvent Caspase-3/7 Green MitoProbe $DiOC_2(3)$ MitoProbe JC-1 YO-PRO-1 Iodide	CellTrace CFSE Click-iT Plus EdU Alexa Fluor 488	CellROX Green	pHrodo Green *E. coli* BioParticles Conjugate pHrodo Green *S. aureus* BioParticles Conjugate	EGFP Emerald GFP EYFP	BD Horizon BB515
	574/26 575/30 580/23 585/40 586/15 590/40	BL2 574/26 BL2 (G,Y‡) 590/40	PE PE-eFluor 610 PE-Alexa Fluor 610 PE-Texas Red	LIVE/DEAD Fixable Red	7-AAD Propidium Iodide (PI) SYTOX AADvanced SYTOX Orange	Vybrant DyeCycle Orange	FxCycle PI/RNase	Annexin V, PE TMRE TMRM MitoProbe JC-1			pHrodo Red *E. coli* BioParticles Conjugate pHrodo Red Phagocytosis Kit	EYFP mCitrine Venus	BD Horizon PE-CF594 PE/Dazzle 594
	670/30 675/30 680/30 695/30 695/40 710/50	BL3 695/40	PerCP-eFluor 710 PE-Alexa Fluor 700 PE-Cy®5.5 PerCP PerCP-Cy®5.5 Qdot 705 TRI-COLOR (PE-Cy®5)		7-AAD Propidium Iodide SYTOX AADvanced			Annexin V, PerCP-eFluor 710					PerCP-Vio700
	750 LP 775/50 780/40 780/60	BL4 780/60	PE-Cy®7 Qdot 800			Vybrant DyeCycle Ruby		Annexin V, PerCP-eFluor 710					PE-Vio770
Green (532 nm)	555/20 575/24 585/16 585/42 610/20	GL1 575/36	Alexa Fluor 532 Alexa Fluor 555 Qdot 565 Qdot 605 R-phycoerythrin (R-PE, PE)		SYTOX Orange	Vybrant DyeCycle Orange		Annexin V, R-PE Annexin V, Alexa Fluor 555 MitoTracker Orange CMTMRos	CellTrace Yellow	CellROX Orange	pHrodo Red *E. coli* BioParticles Conjugate	DsRed tdTomato YFP	
	610/20 620/15 630/30	GL2 620/15	Alexa Fluor 568 Alexa Fluor 594 Qdot 605 PE-Texas Red	LIVE/DEAD Fixable Red	SYTOX AADvanced Propidium Iodide	Vybrant DyeCycle Orange	FxCycle PI/RNase	Annexin V, Alexa Fluor 568 Annexin V, Alexa Fluor 594 MitoTracker Red CMXRos	Click-iT Plus EdU Alexa Fluor 594			mCherry	PE/Dazzle 594
	695/40 710/50	GL3 695/40	Qdot 705 PE-Alexa Fluor 700 TRI-COLOR PE-Cy®5.5		SYTOX AADvanced	Vybrant DyeCycle Ruby							
	780/60	GL4 780/60	Qdot 800 PE-Cy®7										
Yellow (561 nm)	585/40 585/15 590/40	YL1 585/16	Alexa Fluor 555 PE		Propidium Iodide SYTOX Orange	Vybrant DyeCycle Orange		MitoTracker Orange CMTMRos MitoTracker Red CMXRos TMRE TMRM	CellTrace Yellow	CellROX Orange	pHrodo Red *E. coli* BioParticles Conjugate	mOrange RFP	
	610/20 613/20 615/50 620/15 620/30	YL2 620/15	PE-eFluor 610 PE-Alexa Fluor 610 PE-Texas Red	LIVE/DEAD Fixable Red	7-AAD Propidium Iodide SYTOX AADvanced SYTOX Orange	Vybrant DyeCycle Orange	FxCycle PI/RNase	Annexin V, Alexa Fluor 568 Annexin V, Alexa Fluor 594	Click-iT Plus EdU Alexa Fluor 594			DsRed mCherry mKate mStrawberry tdTomato	ECD BD Horizon PE-CF594 PE/Dazzle 594 PE-Vio 615
	670/30 675/30 680/30 695/30 695/40	YL3 695/40 YL3 (B§/Y/R††/V6) 780/60	PE-Alexa Fluor 700 PE-Cy®5.5 Qdot 705 TRI-COLOR		7-AAD Propidium Iodide SYTOX AADvanced							mPlum mRaspberry mNeptune	
	750 LP 780/40 780/60	YL4 780/60	PE-Cy®7 Qdot 800			Vybrant DyeCycle Ruby							PE-Vio770
Red (637 nm)	660/20 661/20 665/20 670/14 670/30 675/30	RL1 670/14	Alexa Fluor 647 eFluor 660 APC Qdot 655 APC-Cy®5	LIVE/DEAD Fixable Far Red	SYTOX Red		FxCycle Far Red	Annexin V, Alexa Fluor 647 Annexin V, Alexa Fluor 680 Annexin V, APC MitoProbe $DiIC_1(5)$ TO-PRO-3	CellTrace Far Red Click-iT Plus EdU Alexa Fluor 647	CellROX Deep Red			
	720/30 730/45	RL2 720/30	Alexa Fluor 680 Alexa Fluor 700 APC-Alexa Fluor 750 Qdot 705										
	750 LP 775/50 780/40 780/60	RL3 780/60	APC-eFluor 780 APC-Alexa Fluor 750 APC-Cy®7	LIVE/DEAD Fixable Near-IR		Vybrant DyeCycle Ruby							BD APC-H7 APC-Vio770

*Filter sets change depending on the configuration of the Attune NxT Flow Cytometer in use. **V6 is the Attune NxT violet 6-channel configuration option.
†G refers to the green laser option. ‡Y refers to the yellow laser option. §B refers to the blue laser option. ††R refers to the red laser option.

To find out more about Invitrogen™ antibodies, assays, and instruments for flow cytometry, go to **thermofisher.com/flowcytometry**

ThermoFisher SCIENTIFIC